Renewable and Sustainable Energy Reviews 65 (2016) 1079–1097

Contents lists available at ScienceDirect

Renewable and Sustainable Energy Reviews

journal homepage: www.elsevier.com/locate/rser

Cooling potential and applications prospects of passive radiative cooling in buildings: The current state-of-the-art

Xing Lu, Peng Xu *, Huilong Wang, Tao Yang, Jin Hou

Department of Mechanical and Energy Engineering, Tongji University, Shanghai 201804, China

ARTICLE INFO

Article history:
Received 21 December 2015
Received in revised form
1 June 2016
Accepted 12 July 2016

Keywords:
Passive radiative cooling
Building integration
Cooling potential
Energy conservation
Mathematical models
Review

ABSTRACT

The universe can be utilized as a sink for heat pumping by means of passive radiative cooling (PRC). This approach is an age-old cooling practice that has had a renaissance with increasing numbers of research papers over the past two decades. This paper reviews the trends of this technique, as well as advancements in recent years, with an attempt being made to analyze the cooling magnitude and developmental prospects for both diurnal and nocturnal periods. The models and calculations for computing the performances of passive radiative cooling systems are discussed along with the designs and fabrication factors that influence a system's performance. Optimizing strategies that maximize the net cooling power are also presented. The various system configurations that are available to date are summarized to demonstrate the building integration forms of PRC systems. The cooling potentials of different systems are assessed by simulations, and it is shown that the daytime cooling energy density is rather modest, even under the most favorable conditions. The barriers that likely exist to widespread application as well as the scopes for further improvements of PRC are also provided. It is noted that the commercialization of PRC systems is primarily limited by coating material constraints and technique reliability. The advent of a new type of material will be a critical solution to the prevalence of PRC.

Contents

* Correspondence to: Department of Mechanical and Energy Engineering, Tongji University, Room A434, No. 4800 Cao'an Road, Shanghai 201804, China.
E-mail address: xupengwb@gmail.com (P. Xu).

http://dx.doi.org/10.1016/j.rser.2016.07.058
1364-0321/

1. Introduction

Cooling is a high-energy-consuming practice that is embarked upon by modern societies, and it is also a dominant driver for daytime demand peaks and overloaded grids [1]. As a rule of thumb, approximately 40% of primary energy is used in buildings, and the major energy consumption is allocated to conventional HVAC systems [2]. A passive cooling technique that cools with no power input or little power input could therefore make a tremendous difference in energy conservation and emissions reduction. Such strategies do not need to cover all of the cooling loads of a space, but should be able to ease the reliance on conventional systems. Passive radiative cooling (hereinafter PRC) possesses enticing potential for reducing energy use in buildings and is one of the viable alternatives in this regard.

Beyond the earth's atmosphere, the void of space has an extremely low temperature, which is close to absolute zero [3]. Cooling would be a straightforward matter if it were possible to harness the cold darkness of the universe as a heat sink, with the atmosphere interposed between us and this potential cooling source. The semi-transparent nature of the atmosphere is conducive to the imbalance of incoming and outgoing energy and could allow for a sub-ambient cooling phenomenon.

Radiative cooling is a common phenomenon at the earth's surface, and it can be illustrated by processes that abound in nature, such as dew and frost formation on plants. Its application is also extensive over many domains: Dew water collection in remote areas is one of the embodiments [4]; collecting coolness via radiative cooling can boost the efficiency of the power output of turbines or other power thermal systems [5]; and radiatively lowering the operating temperature of a solar cell through sky access is an effective way to enhance the efficiency of the cell [6]. However, in this paper, the synergies of PRC with buildings are the main focus.

The cooling potential of PRC in buildings was first utilized by societies in 400 BCE. Night sky cooling was used in the yakh-chal to produce ice by Persians, despite higher ambient air temperatures [7]. Similar ingenious applications have been used in the desert of Chile and with ice pits in the West Indies [8]. From the mid-20th century, various architectural forms and living practices have utilized radiative cooling effects, and nocturnal radiative cooling of buildings has increasingly attracted considerable research [9]. Exposed sleeping areas in courtyards and on rooftops make it possible to reject heat directly to the sky and simultaneously to obtain the advantages of cool outdoor air temperatures and breezes, as illustrated in Fig. 1 [10]. Special roof systems, including roof ponds and radiative cooling panels, similar to solar flat plate collectors, are also typical examples. However, the use of nocturnal radiative cooling was somehow abandoned later due to product reliability and advances in other technologies that favored more conventional means of cooling, e.g., vapor compression or vapor absorption systems.

Until the past decade or two, passive radiative cooling has seen a renaissance that is chiefly motivated by the depletion of fossil fuels and concerns about the environment, which can be observed from efforts directed at studies on improving the performance and use of the passive radiative cooling concept. Some of these attempts are seen in the optimization of selective surfaces and cover foils to explore possibilities for both diurnal and nocturnal radiative cooling [11].

To the knowledge of the authors, several review papers exist on the passive cooling of buildings in a number of top energy journals [12–17], whereas the existing literature reviews that merely pertain to the subject of radiative cooling in buildings are either limited or incomplete. Ming et al. [18] briefly analyze the physical and technical potential of radiative cooling to combat climate change macroscopically. M. Hanif et al. summarize one of the calculation methods of determining radiative cooling power, and Nwaigwe et al. enumerate experiments and field tests on different night-time PRC systems [19,20].

In this paper, a comprehensive overview of passive radiative cooling in buildings is performed on the basis of previous studies, and it has a twofold significance. First, basic concepts and the development courses of PRC systems are presented by reviewing trends in published articles and applications. Second, the outcome of this paper could be accessible for researchers, students and manufacturers who work in this field by addressing key issues in terms of system configurations and modeling, cooling potentials, material constraints, weather restrictions and cost issues. Section 2 introduces the models for calculating the magnitudes of the resources. In Section 3, the classification of PRC systems and summaries of various system designs and configurations are presented. In Section 4, the cooling potential and applications prospects of PRC systems are concisely analyzed. Finally, salient concluding remarks are outlined in Section 5.

2. Models and calculations

In this section, models and calculations of PRC are detailed as the foundation of assessing the cooling magnitudes of the various systems. The net cooling power for radiative cooling is subject to outgoing radiative power by the emitting structure (P_{sur}), the amount of atmospheric radiation (P_{atm}), and the solar irradiance (P_{sun}) and convection that is absorbed by the structure (P_{cov}). The overall heat balance of a radiative structure is described in Eq. (1) [21,22,54,136] and illustrated in Fig. 2.

$$P_{rad}(T_s) = P_{sur}(T_s) - P_{sky}(T_{amb}) - P_{sun} - P_{conv} \quad (1)$$

where $P_{rad}(T_s)$ represents the net radiative cooling power at the surface temperature T_s. $P_{sur}(T_s)$ is the power that is radiated by the surface at the temperature T_s. $P_{sky}(T_{amb})$ is the incident atmospheric radiative power at the ambient temperature. P_{sun} represents the incident solar power that is absorbed by the surface in the daytime. The convection heat transfer is denoted by P_{conv}.

Each item will be elucidated in the following sections, and the optimum strategies for achieving the maximum overall net power are further discussed in Section 2.4.

Nomenclature

P_{rad}	net radiative cooling power (W/m^2)
P_{sur}	power radiated by the surface (W/m^2)
P_{sky}	incident atmospheric radiative power (W/m^2)
P_{sun}	incident solar power absorbed by the surface in the daytime (W/m^2)
P_{conv}	convection heat transfer power (W/m^2)
T_s	surface temperature (K)
T_{amb}	the ambient temperature (K)
T_{dp}	dew point temperature (K)
T_{sky}	equivalent sky temperature (K)
T_a^*	effective sky temperature (K)
ε_{sky}	sky emissivity
ε_s	surface emissivity
ε_{cs}	equivalent atmospheric emissivity under clear sky
$\varepsilon(\lambda, \theta)$	spectral and angular emissivity
$\varepsilon(\lambda, \theta_{Sun})$	wavelength-dependent emissivity of the sun
$\varepsilon_{sky}(\lambda, \theta)$	wavelength and angle-dependent emissivity of the atmosphere
$I_{AM1.5}(\lambda)$	solar illumination (W/m^3)
$I_{BB}(T, \lambda)$	spectral radiance of a black body ($W/(m^3\ sr)$)
e_{amb}	evaporation pressure of the ambient air (Pa)
A	area of the surface (m^2)
λ	wavelength (m)
Ω	angular coefficient (sr)
θ	the angle from the zenith (deg)
h	Planck's constant
k_B	Boltzmann constant
σ	Stefan-Boltzmann constant ($W/m^2\ K^4$)
c	speed of light (m^2/s)
$P(T, \lambda)$	hemispherical spectral radiance of a black body ($W/(m^3\ sr)$)
h_c	combined non-radiative heat coefficient that captures the collective effects of convection and conduction ($W/(m^2\ K)$)

2.1. Infrared radiative heat transfer

Radiative heat transfer has two components: thermal emission to the full sky hemisphere and absorption of radiation emitted by the atmosphere. The calculation methods of these two terms can be divided into the selective-dependent approach and the selective-independent approach, and the relationship between the two approaches is explained in the following section.

2.1.1. Selective-dependent approach

The outgoing radiation term emitted by the structure can be physically described by Eq. (2). The equivalent forms are also given by Hossain et al. [21] in Eq. (3) and Gentle et al. [22] in Eq. (4).

$$P_{sur}(T) = \int d\Omega \cos\theta \int_0^\infty d\lambda I_{BB}(T, \lambda)\varepsilon(\lambda, \theta) \tag{2}$$

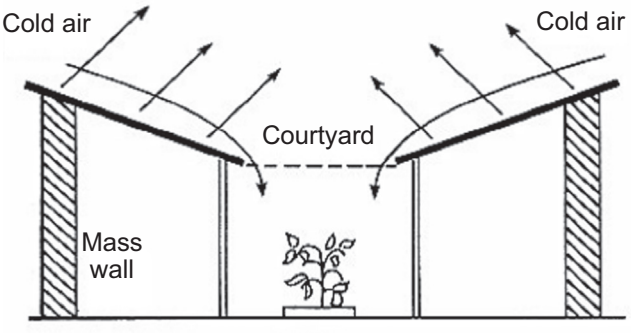

Fig. 1. Schematic of an ancient building with an enclosed courtyard [10].

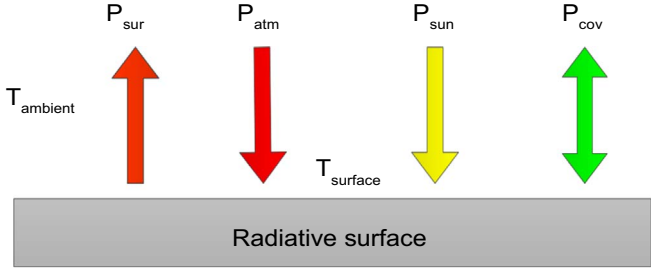

Fig. 2. Composition of energy flows into and through a radiative structure.

where θ is the angle from the zenith. $\int d\Omega = 2\pi \int_0^{\frac{\pi}{2}} d\theta \sin\theta$ is the angular integral over a hemisphere. $I_{BB}(T, \lambda) = \frac{2hc^2}{\lambda^5} \frac{1}{e^{hc/(\lambda k_B T)} - 1}$ is the spectral radiance of a black body defined by Planck's law at any temperature T, and $\varepsilon(\lambda, \theta)$ is the spectral and angular emissivity.

$$P_{sur}(T) = \int_0^{\pi/2} \pi \sin 2\theta d\theta \int_0^\infty d\lambda I_{BB}(T, \lambda)\varepsilon(\lambda, \theta) \tag{3}$$

$$P_{sur}(T) = \int_0^{\pi/2} d(\sin^2\theta) \int_0^\infty d\lambda P(T, \lambda)\varepsilon(\lambda, \theta) \tag{4}$$

where $P(T, \lambda) = \frac{2\pi hc^2}{\lambda^5} \frac{1}{e^{hc/(\lambda k_B T)} - 1}$ is the hemispherical spectral radiance of a black body.

The incoming radiation term from the atmosphere is calculated as the integral formula in Eq. (5).

$$P_{sky}(T_{amb}) = \int d\Omega \cos\theta \int_0^\infty d\lambda I_{BB}(T_{amb}, \lambda)\varepsilon_{sky}(\lambda, \theta)\varepsilon(\lambda, \theta) \tag{5}$$

where $\varepsilon_{sky}(\lambda, \theta)$ is the wavelength and angle-dependent emissivity of the atmosphere.

The spectral distribution of the sky radiation is quite similar to that of a black body at a temperature that is equal to the dry bulb temperature of the air near the ground, except in the spectral region of 8 μm to 13 μm. This part of the spectrum, which is known as the 'atmospheric window', is nearly transparent to infrared radiation – if the atmosphere is very dry. It is also necessary to account for the continuous drop in the transparency across this sky window for ray directions that are at angles θ to the vertical. The spectral radiance of the atmosphere was measured at Coco Beach, Florida, by Bell et al. [23], and it shows the radiance of the atmospheric window at various angles from the zenith compared to the radiance of a black body at 298 K, as depicted in Fig. 3.

It can be concluded from above that the atmospheric radiation has two distinctive features: first, the atmosphere appears to be complete 'black' at Planck wavelengths that are outside of the 7.9 μm to 13 μm range.

Second, the atmosphere is increasingly 'black' at higher angles to the zenith between 7.9 μm and 13 μm. Based on those characteristics, under a clear, dry sky, a useful approximation to the θ-dependent change in $\varepsilon_{sky}(\lambda,\theta)$, which is largely confined to the sky window band, is given by Eq. (6) for λ between 7.9 μm and 13 μm. The remainder of the Planck spectrum, where the atmosphere is assumed to be "black" with $\varepsilon_{sky}(\lambda,\theta) = 1.0$, is given by Eq. (7) [24].

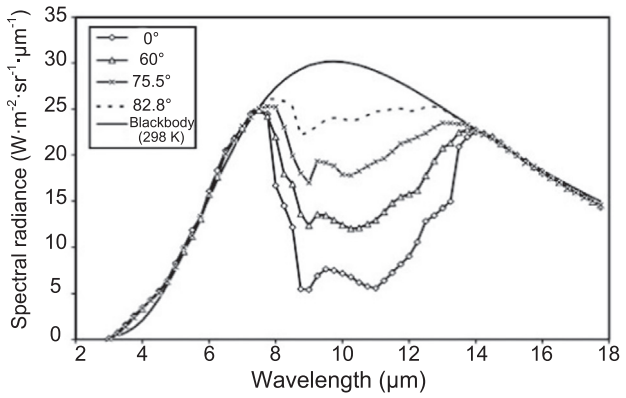

Fig. 3. Spectral radiance of the atmosphere measured at Coco Beach, Florida, compared to the radiance of a black body at 298 K [23].

Another similar model for $\varepsilon_{sky}(\lambda,\theta)$ is given by Eq. (8), where $t(\lambda)$ is the atmospheric transmittance in the zenith direction, which is modeled from software such as Modtran, PcModWin [25].

$$\varepsilon_{sky}(\lambda,\theta) = 1 - 0.87^{1/\cos\theta} \quad 7.9\ \mu m < \lambda < 13\ \mu m \tag{6}$$

$$\varepsilon_{sky}(\lambda,\theta) = 1.0 \qquad \lambda < 7.9\ \mu m,\ \lambda > 13\ \mu m \tag{7}$$

$$\varepsilon_{sky}(\lambda,\theta) = 1 - t(\lambda)^{1/\cos\theta} \tag{8}$$

2.1.2. Spectral and angular selectivity

As shown in the above integral equations, θ and λ are the two governing factors, which demonstrate the spectral and angular selectivity of a radiative surface. In the early years, radiators were mostly built with a highly emissive grey body in the hope of radiating out more power in a continuous broad band. With the development of nanotechnology, manipulating the spectral and angular selective properties of a surface opened a wider scope for the PRC. The spectral and directional absorption profile of a selective emittance surface is shown in Fig. 4.

The infrared spectral properties of an emitting surface have a significant impact on the radiated energy. For a black body emitter at temperature T, all of the wavelengths emit energy at the maximum possible as dictated by the Planck blackbody radiation spectra at T. Alternatively, if a surface has an ε(λ) value that is much higher at some wavelengths than at others, a selective emitter is achieved. If an emitting surface is produced with an emittance profile that is complementary to that in the sky window, it is possible to continue to have a net output of energy at sub-ambient temperatures that is lower than those that can be attained by a black body [26].

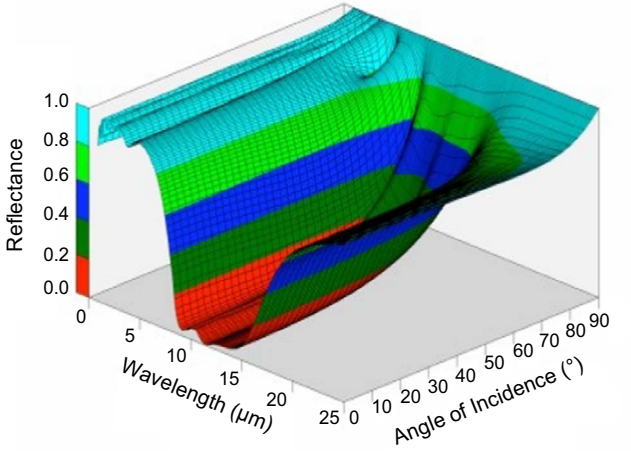

Fig. 4. Spectral and directional absorption profile of a selective emittance surface [26].

Angular selectivity is utilized on the basis of the unique features of the atmospheric radiation mentioned in Section 2.1.1, to reduce the incoming absorbed radiation from the sky. Several studies on PRC using angular selective approaches have been reported. Multilayer thin films are designed to yield increased infrared reflectance as the angle of incidence increases [27]. Fig. 5 exhibits specular spectral reflectance at various angles of incidence onto an a-SiC/SiO multilayer, while radiating predominantly near the zenith through the sky window; the ideal net radiative output is reported to reach 118 W/m^2. Heat mirror apertures are another set-up that uses angular selectivity to amplify radiative cooling [28]. This set-up also ensures that any incident radiation from directions that are closer to the horizontal is much less than that from the same directions in the atmosphere. The schematics of an external mirror are shown in Fig. 6. The two mirrors are composed of low emissive surfaces, while the radiative coatings can be sky window selective or highly emissive material. The mathematical model of the optic system is expressed in Eq. (9). The outgoing term remains almost unchanged, and the first incoming term represents the atmospheric radiation from 0 to θ_{max}. It is worthwhile to note that the second incoming term will drop off if the heat mirrors approach ideal ($\varepsilon_{mirror}=0$). Compared to the angular selective material, more radiation goes out in the case of a mirror for which the spectral properties of the coating do not change very much with the angle of incidence.

$$P_{rad} = \left[\int_0^{\pi/2} d(\sin^2\theta)\int_0^{\infty} d\lambda P(\lambda, T_s)\varepsilon_s(\theta,\lambda)\right] - \left[\int_0^{\theta_{max}} d(\sin^2\theta)\int_0^{\infty} d\lambda P(\lambda, T_{amb})\varepsilon_{amb}(\theta,\lambda)\varepsilon_s(\theta,\lambda)\right] - \left[\int_{\theta_{max}}^{\pi/2} d(\sin^2\theta)\int_0^{\infty} d\lambda P(\lambda, T_{amb})\varepsilon_{mirror}(\theta,\lambda)\varepsilon_s(\theta,\lambda)\right] \tag{9}$$

2.1.3. Selective independent approach

Atmospheric radiation (P_{sky}) is emitted approximately in the range of 4–100 μm, mainly by H_2O, CO_2, and O_3 molecules and cloud water droplets [29]. Due to the complexity of testing these components, various statistical correlations have therefore been proposed between P_{sky} and meteorological parameters that are measured on a widespread basis, which could be used as surrogates for atmospheric emissivity, as listed in Table 1. In Eq. (10), we assume the sky to be a grey body that has a temperature equal to the ambient dry bulb temperature, in which case the differences in radiation emitted due to variations in the atmospheric moisture content are accounted for by modifying the sky emissivity ε_{sky}.

$$P_{sky} = \varepsilon_{sky}\sigma T_{amb}^4 \tag{10}$$

where T_{dp} is the dew point temperature, T_{amb} is the dry-bulb temperature in the ambient, and e_{amb} is the evaporation pressure of the ambient air.

With the clouds becoming dense and opaque, the water vapor has a significant impact on the longwave radiation, which leads to an increase in the average atmospheric emissivity. Research on corrections to the equivalent sky emissivity has been performed by many scholars, as tabulated in Table 2.

where c is the cloud fraction, which can be obtained from visual observations [46,47] from solar radiation measurements [48] or occasionally from satellite data [49].

The outgoing radiation that is given off by the surface (P_{sur}) can be calculated by introducing the weighted average hemispherical emissivity, as shown in Eq. (11). The ε_s equals 1.0 for a black body

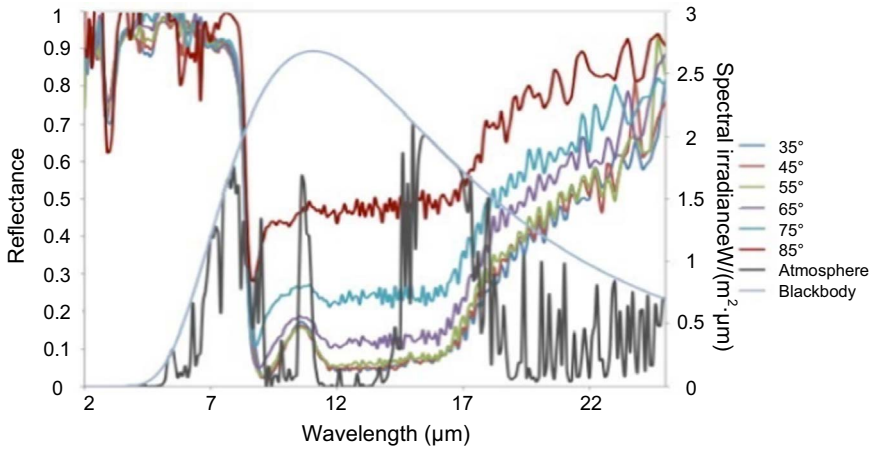

Fig. 5. Specular spectral reflectance at different incident angles onto an a-SiC/SiO multilayer [27].

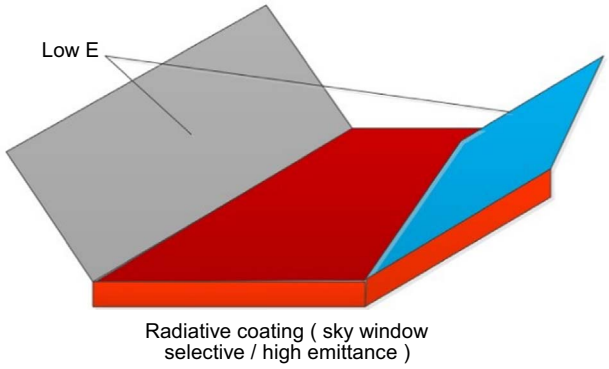

Fig. 6. Schematics of an external heat mirror aperture [27].

Table 1
Formulas of equivalent atmospheric emissivity under clear sky.

Author	Correlation	Year
Bliss [30]	$\varepsilon_{cs} = 0.8004 + 0.0396T_{dp}$	1961
Swinbank [31]	$\varepsilon_{cs} = 9.36 \times 10^{-6} \times T_{amb}^2$	1963
Idso and Jackson [32]	$\varepsilon_{cs} = 1 - 0.261 \exp\left[-7.77 \times 10^{-4} \times (273 - T_{amb})^2\right]$	1969
Brutsaert [33]	$\varepsilon_{cs} = 1.24 \times \left(e_{amb}/T_{amb}\right)^{1/7}$	1975
Clark and Allen [34]	$\varepsilon_{cs} = 0.787 + 0.0028T_{dp}$	1978
Idso [35]	$\varepsilon_{cs} = 0.7 + 5.95 \times 10^{-5} e_{amb} \exp(1500/T_{amb})$	1981
Berger et al. [36]	$\varepsilon_{cs} = 0.770 + 0.0038T_{dp}$	1984
Berdahl and Martin [37]	$\varepsilon_{cs} = 0.711 + 0.56\frac{T_{dp}}{100} + 0.73(\frac{T_{dp}}{100})^2$	1984
Chen et al. [38]	$\varepsilon_{cs} = 0.736 + 0.00571T_{dp} + 0.331810^{-5}T_{dp}^2$	2010

Table 2
Modified formulas of equivalent atmospheric emissivity under cloudy sky.

Author	Correlation	Year
Maykut and Church [39]	$\varepsilon_{sky} = (1 + 0.22c^{2.75})\varepsilon_{cs}$	1973
Jacobs [40]	$\varepsilon_{sky} = (1 + 0.0.26c)\varepsilon_{cs}$	1978
Kasten and Czeplak [41]	$\varepsilon_{sky} = \varepsilon_{cs} + 0.8(1 - \varepsilon_{cs})\left[1.4286(G_d/G) - 0.3\right]^{0.5}$	1980
Berdahl and Martin [42]	$\varepsilon_{sky} = \varepsilon_{cs} + (1 - \varepsilon_{cs})n^{(-h/h_0)}\varepsilon_{cloud}$	1984
Martin [43]	$\varepsilon_{sky} = \varepsilon_{cs} + (1 + 0.0024n + 0.0035n^2 + 0.00028n^3)$	1989
Sugita and Brutsaert [44]	$\varepsilon_{sky} = (1 + 0.0496c^{2.45})\varepsilon_{cs}$	1993
Lhomme et al. [45]	$\varepsilon_{sky} = (1.03 + 0.34c)\varepsilon_{cs}$	2007

and represents the fraction of the total energy under the Planck spectrum within the range 7.9–13 mm for an 'ideal emitter'.

$$P_{sur} = \varepsilon_s \sigma T_s^4 \tag{11}$$

In fact, all of the practical radiators can be recast in the generic non-selective form shown in Eq. (12) to describe the radiative heat transfer process except that the temperature that defines the average hemispherical surrounds is no longer T_{amb} but an effective sky temperature T_a*, which depends on the spectral and angular properties of the emitting surface. In other words, the impact of the sky window is to reduce the incoming intensity below that of a black hemisphere at T= T_{amb} to that at a lower effective sky temperature T_a*.

$$P_{rad} = \varepsilon_s \sigma \left[T_s^4 - \left(T_a^*\right)^4\right] \tag{12}$$

The selective independent approach addresses only the total flux of radiant energy, which is assumed to have a continuous spectrum irrespective of the actual spectral distribution of the outgoing and incoming radiation. Thus, it is more suitable for radiative surfaces that can be regarded as grey and Lambertian surfaces. Many approximations of the net radiative heat transfer can be finally reduced to Eq. (12). For example, the relationship expressed in Eq. (13) by Dimoudi et al. [50] and the linearized form of the Stefan-Boltzmann Law shown in Eq. (14) by Martin are widely used in the modeling of a radiative cooling panel [43].

$$P_{rad} = \varepsilon_s \sigma [T_s^4 - (1 + 0.0224n - 0.0035n^2 + 0.00028n^3)^* \varepsilon_{sky} T_{amb}^4 \tag{13}$$

where n is the total opaque cloud amount, which is 0 for clear sky and 10 for overcast sky.

$$P_{rad} = 4\varepsilon_s \sigma T_{amb}^3 \left[T_s^4 - T_{sky}{}^4\right] \tag{14}$$

where T_{sky} is the equivalent sky temperature.

2.2. Solar radiation

The solar radiation part can be expressed by Eq. (15), where the solar illumination is represented by $I_{AM1.5}(\lambda)$, the AM1.5 spectrum. The term P_{Sun} does not have an angular integral because the radiator is assumed to face a fixed angle θ_{Sun}.

$$P_{sun} = A \int_0^\infty d\lambda \varepsilon(\lambda, \theta_{sun}) I_{AM1.5}(\lambda) \tag{15}$$

This part is considered only in the calculation of daytime radiative cooling. Daytime radiative cooling is difficult to realize due to high solar radiation intensity. In early years, moving insulation

panels were used to curb the penetration of the solar radiation. Highly reflective roofs were installed to absorb less heat during the day. Recently, selective multi-layers that have low emissivity in the solar spectrum and high emissivity in the sky window are available and make cooling possible during the daytime [11].

2.3. Convection heat transfer

In most cases, the convection heat transfer between the surface and the adjacent air have a negative effect on the PRC and cannot be neglected. The heat transfer function is shown in Eq. (16), where h_c is a combined non-radiative heat coefficient that captures the collective effects of convection and conduction. Several experiments have been conducted to evaluate this quantity, and different empirical formulas were developed under various circumstances [50–52]. In some research, h_c is determined by using software such as FLUENT or COMSOL [53,54].

$$P_{conv}(T_s, T_{amb}) = h_c(T_{amb} - T_s) \quad (16)$$

The sub-ambient temperature of the selective surface prompts us to take caution to hinder the effect of the convection, and there are two major solutions: 1) Wind covers and 2) Wind shields.

2.3.1. Wind covers

An ideal wind cover is used to suppress the convective heat flux from warm air that reaches the surface, and it possesses several unique attributes: high IR transmittance, mechanical strength, low cost and long-term outdoor durability. However, materials that are suitable for use as convection covers are much more difficult to identify [55]. Table 3 tabulates the key properties of the existing convection cover materials. Polyethylene film has been widely employed in a proof-of-concept stage, despite its vulnerability to damage by solar ultraviolet radiation [56]. Inorganic and semiconductor alternatives such as ZnS, ZnSe and Silicon are considered to be durable substances but are to date far too expensive. High-density polyethylene mesh over a large area (roof) has been demonstrated to be feasible experimentally and with simulation models by Gentle et al. [57]. A set of novel mesh covers manifest significant convection suppression and enhanced night sky radiative cooling. Notably, they are most sensitive to the magnitude and sign of the difference between the roof temperature and ambient temperatures but not sensitive to the wind velocity. Currently, the research is confined to only high emittance surfaces.

2.3.2. Wind shield

A wind shield is also intended to reduce the convective heat transfer by placing shield walls all around, which is more weather proof than a wind cover. The effect of a wind shield has been studied by CFD calculations and by wind tunnel experiments under conditions that are appropriate for the climate of Thailand [53]. The first major effect is on convective heat transfer. Higher wind barriers give useful reductions in the convection because a low wind shield increases the turbulence over the surface, but higher wind shields cause a separation of the main airflow from the surface. The second major effect is the radiative heat exchange between the wind shield and the radiative surface. Increasing the wind shield height could interfere with radiative cooling from the radiative surface. Atmospheric radiation from directions near the horizontal must also be accounted for, in which the emittance of the wind shield and its solid angle projection onto the surface being cooled are two factors that are of concern.

Table 3
Key properties of potential convection cover materials [55–57].

Material	Mean transmittance 8–13 μm	Toxicity	Solar damage	Cost
Polyethylene	73% (100 μm thick)	Non-toxic	Yes	Low cost
ZnS	64% (4 mm thick)	Low	No	High cost (if high purity)
ZnSe	70% (7.1 mm thick)	Hazardous by skin contact	No	High cost
Silicon	47%(0.6 mm thick)	Non-toxic	No	High cost
HDPE mesh	80% (100 μm thick)	Non-toxic	No	Low cost

2.4. Optimizing strategies to achieve the maximum net output

In this section, the optimizing strategies to enlarge the net radiative cooling effect are analyzed from each term of the basic physical model.

From Eqs. (2,5) and (16), we can determine the dictating factors that influence the maximum net output: the temperature of the radiator surface (T_s), the ambient air (T_a), and the emissivity of the radiator (ε_s) and the atmosphere (ε_a). T_a and ε_a are fixed for a certain region, while T_s is closely related to the design purpose of the PRC system, for building load reduction or water cooling. The emissivity properties of a surface are the issue that we can choose and manipulate.

Fig. 7(a) is derived from the experimental results in [25,58] and shows the net radiated power and convection heat transfer power of a spectral selective surface and a highly emissive surface under different temperature depressions. It can be observed that when the difference between Ta and Ts is small, the highly emissive surface has a higher net cooling rate; however, when Ts falls, the spectral selective surface is preferred. Fig. 7(b) is the schematics of the system for water cooling. The heat transfer between the water and the surface is described as $P(T_s, T_f) = Ah(T_f - T_s)$, where T_f is the average temperature of the cooling water. The crossover of the radiated power curve and the convection power curve is the system balance point. It can be concluded that when T_f is high under a steady state, the highly emissive surface can radiate out more energy, while the spectral selective surface is better suited to use when T_f is low. In other words, a non-selective emitter is preferable because it allows for maximum cooling just below and above the ambient temperature. A selective emitter coating is better for cases in which a greater sub-ambient temperature for the produced water is desired.

The emissivity profile of the atmosphere is easily influenced by the humidity and the air pollution conditions. The different pollutants have complicated interference with long-wave sky radiation, and because of the complexity, we will not discuss it here. However, it is verified that a highly emissive surface has a greater advantage when the humidity is relatively low [58].

When using the heat mirrors that were mentioned above, low emissivity must be guaranteed. Especially for the highly emissive non-selective surface, the heat mirrors are more appropriate to use due to the significant reduction in the atmospheric radiation at large angles.

With regard to being cautious about reducing the convection, the tradeoff for the outgoing radiation must be considered. For example, the wind cover and mesh hinder certain portions of the IR transmission, and higher wind shields can interfere with the radiation transfer at the surface. Thus, the measures are better taken under large wind velocities or a large temperature depression between T_a and T_s.

3. Classification and system configuration

Passive radiative cooling can be classified into nocturnal cooling and daytime cooling according to the operating periods. The applications of nocturnal radiative cooling are well developed, while daytime radiative cooling is still an emerging field.

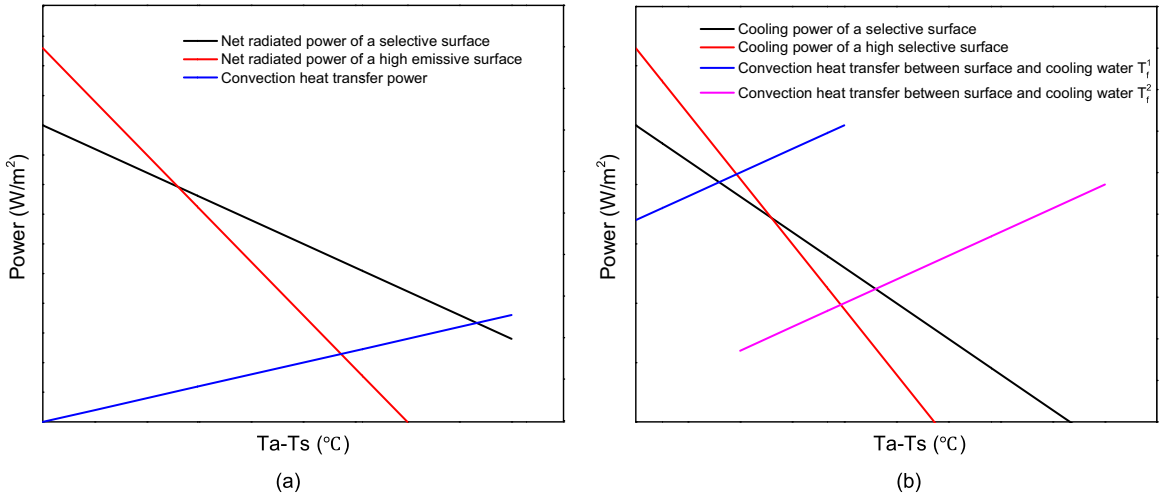

Fig. 7. The relationship between the power and the temperature depression of Ta-Ts.

3.1. Nocturnal cooling

One of the pioneering applications that was integrated into the building sector was traced back to approximately 60 years ago, when a few experimental single-story buildings in the US were cooled by long-wave radiation by means of removing the thermal insulation during summer nights, to expose a roof pond or a massive roof [59]. Such systems are called 'Movable insulation',

Table 4
Correlations of different system configurations of PRC.

System Type	Open water-based	Closed water-based	Air-based
Advantages	• Provide both heating and cooling with the same components. • Performance is independent of building orientation. • Desirable performance to maintain stable indoor temperature under favorable climate conditions.	• Use of conventional components. • Can be retrofitted over existing flat roof at low cost. • Water is a far more effective heat transfer medium than air which results in less contact area.	• Use of conventional components. • Can be retrofitted over existing flat roof at low cost. • Air does not freeze and leakage is far less critical than a water leakage.
Disadvantages	• Lack of experience by the construction industry. • The roof must support a load of 200–400 kg/m^2	• Must be laid flat or slighted pitched. • May require provision of a specially designed cool store. • Radiators need to be coupled to cooling panels acting as interim heat stores for buildings of more than one storey.	• Must be laid flat or slighted pitched. • May require provision of a specially designed cool store. • Requires a far greater contact area for heat transfer than water does. • Radiators need to be coupled to cooling panels acting as interim heat stores for buildings of more than one storey.
Impact factors	**Uncovered** • Reflectance of pond floor • Water depth**Covered** • Thermal conductance and emissivity of cover • Solar absorptance and transmissivity of cover • Air space between cover and pond • Physical properties and operation of pond cover	• The coupling of the building with the emitter. • Environmental conditions (e.g. atmospheric humidity, cloud cover). • Radiative material &color • Pipe diameter, length & spacing • Back insulation • Windscreen • Storage mass • Inlet water temperature • Water flow rate	• The coupling of the building with the emitter. • Environmental conditions(atmospheric humidity and cloud cover). • Thickness & length of air space • Pipe diameter, length & spacing • Back insulation • Windscreen • Storage mass • Inlet air temperature • Air flow rate
Suggestions	• Water depth should be at least 300 mm. (Uncovered) • The emissivity of the radiative surface should be chosen with discretion, for it has negligible effect. • The absorptance of the opaque cover and ventilation of airspace between cover have little influence on performance.	• Dark if used as backup heating system, otherwise light. • Pipe diameter should be appropriate for required flow rate. Length suited to roof dimensions. Pipes as closely spaced as possible. • Back insulation and windscreen are required if the water is cooler than ambient temperature, otherwise their effects are contradictory. • Storage mass either water reservoir or concrete cooling panels. • Water flow should be slow when low outlet temperature is required and should be relatively high if maximum cooling is in demand.	• Highly conductive metal sheet. • Air gap 1–2 cm. Length limited by friction and power of fans. • Back insulation and windscreen are required. • Storage mass either rocks or concrete cooling panel. • Air speed less than 7 m/s

and their major disadvantage lies in the mechanism that is installed to move and replace the bulky insulation panels.

In subsequent decades, a considerable amount of research delved into the application of nocturnal cooling in buildings. Based on the heat-exchange medium, the research can be divided into water-based systems and air-based systems. In addition, researchers investigate the novel hybrid systems for either standalone heat pumping or complementing conventional cooling systems under different climate conditions. Each of these specific system designs will be discussed in the following section. The correlations of the different system configurations are also summarized in Table 4.

3.1.1. Water-based systems

Water-based systems, as the name implies, utilize water as a heat transfer fluid to achieve the desired cooling.

Open water-based systems, which are exemplified by roof pond systems, have been investigated widely in arid regions. This technique, as shown by a typical system design with mechanical ventilation in Fig. 8 [60], is composed of a shallow pond of water on the rooftop, which absorbs heat from the building interior and dissipates it to the surrounding heat sink by radiation and evaporation. Sodha et al. [61] and Nahar et al. [62] investigated experimentally and analytically the water cooling by both evaporation and nocturnal radiation in open roof ponds with movable thermal insulation. Ali [63] performed an experimental and analytical study on nocturnal water cooling water in an uninsulated open tank. Chen et al. set up a model of a roof pond that was coupled directly to a room that had water spraying over a floating coated insulation, and they validated their approach with experiments [64,65]. In a similar vein, nocturnal radiative cooling and the spraying of water was studied analytically by Roberts [66] and experimentally by Sahar [60]. Tang and Etzion [67,68] and Tang et al. [69] analyzed theoretically and studied experimentally the water cooling by the use of night sky radiation and evaporation in a roof pond that had gunny bags (RPWGB) floating on the water surface. To optimize the effectiveness of the RPWGB system, Spanaki et al. marked the parameters that affected the system performance and developed an improved RPWGB system by using a low emissivity textile that was kept afloat at the water level [70]. Spanaki et al. presented a review of twelve roof pond variants for passive cooling purposes, and they analyzed the pros and cons of various roof pond configurations and discussed the criteria for optimal selection of a roof pond design [71]. Although roof ponds could achieve efficient passive cooling, there are still several prominent issues that limit the widespread application of these systems. As Givoni noted, the wet bulb temperature of the ambient air should be lower than 20 °C, which limits the application of

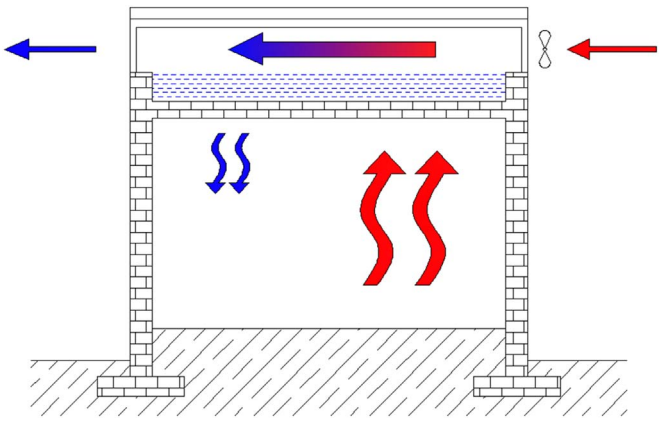

Fig. 8. Schematic diagram of a roof pond system with mechanical ventilation.

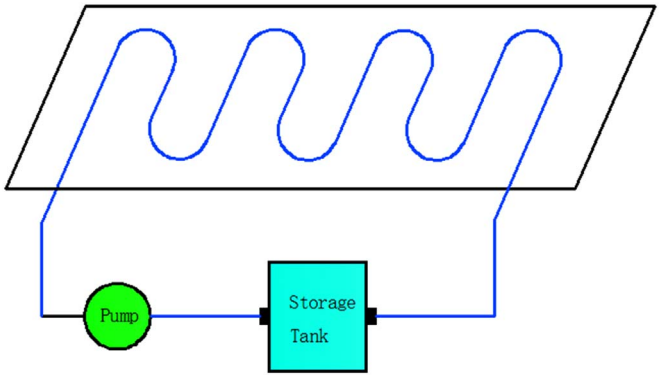

Fig. 9. Schematic diagram of a typical flat-plate radiator system.

such systems to only hot-arid locations [43]. Furthermore, the roofs should be watertight, and they require additional structural strength to support 200–400 kg/m^2. The aesthetics, winter function and maintenance should also be considered.

Closed-water systems are so named because the heat carrier (water) flows through pipes that are embedded in a flat-plate cooling radiator. Usually, these systems consist of a radiative plate, an insulated water tank and a heat pump. Fig. 9 is a simplified schematic diagram of a cooling system that is thus constructed. One of the first applications of such systems was performed by Juchau et al. [72] in 1981, and the concept was further developed by Erell et al. [73] in Israel. Saitoh and Fujino [74] proposed an energy-efficient house that utilized a sky radiator with a large storage tank to store the energy seasonally. The field test results demonstrated that the house consumes only one-sixth of the fossil energy compared with the conventional residence. Argirious et al. [75] assessed the radiative cooling potential theoretically using 12 years of hourly weather data in Athens. Ali H. et al. [3] conducted both experimental and theoretical studies of nocturnal water cooling through a two-parallel-plate radiator unit that was covered by a wind screen. The effect of different factors on the system performance was sketched in the paper, for example, the mass flow rate, uncovered from the ambient versus covered supply warm water tank, and the thickness of the windscreen cover. Similar studies that incorporated theoretical analysis and experimental validation for flat plate radiator systems were conducted by Al-Nimr et al. in Jordan [76,77], Erell et al. in Israel [51,78], Meir et al. in Norway [52], Dimoudi et al. in Greece [50], Hosseinzadeh et al. in Denmark [79], Anderson et al. in New Zealand [80], Okoronkwo et al. in Nigeria [81] and Ferrer et al. in Spain [82].

Water-based systems store energy through nocturnal radiation to provide cold water for daytime cooling. However, the cold water is not sufficiently chilled because the goals of obtaining a lower outlet temperature and pursuing a higher cooling intensity contradict each other, which limits the application of this technique. The heat dissipation of the space undergoes two heat transfer processes—it first transfers heat to the circulated water, which in turn dissipates heat to the sky via the radiator. For these reasons, the water-based systems often integrate with other well-developed technologies, as detailed in Section 2.1.3.

3.1.2. Air-based systems

In an air-based system, the air is flown beneath the surface of a roof-mounted radiator or a cool roof driven by a fan or natural process due to the buoyancy effect before ingress into the building internal mass, to provide instantaneous cooling during the nighttime.

Givoni [83] implemented an earlier roof-mounted air cooler called a ‘roof radiation trap’ in Israel, which was perceived to be impractical with respect to current architectures. A mathematical

model of a lightweight metallic radiator with an air space was built using climatic data in Italy. The cooling output was predicted to vary from 29.7 to 55.8 Wh/m^2 [84]. Another lightweight aluminum nocturnal radiator, painted with an appropriate paint, was established in Greece [85]. Similarly, an analytical model was set up and validated by the extensive comparison of the experimental air temperature values at the radiator's outlet with the theoretical values, where a good agreement was found. Khedari et al. conducted a field investigation of night radiation cooling under Thailand's hot and humid climate in winter. The performances of four types of air-based radiators were tested, and the results showed that the depressions of different surface temperatures were in the range of 1–6 °C below the ambient temperature under both clear and cloudy skies [86]. Work performed by Parker et al. at the Florida Solar Energy Center in 2005–2008 tested the potential of a novel residential night cooling concept, called 'NightCool' (see Fig. 10). This system uses a sealed attic covered by a metal roof that was selectively linked or decoupled by air flow to the home's internal conditioned zone with the attic zone, to provide cooling, and it was supplemented by a desiccant-based dehumidification system and an air conditioner. The delivered seasonal cooling rate averaged approximately 5–10 W/m^2 of the roof surface on an average evening, which was rather modest [87,88]. Canada's National Solar Test Facility (NSTF) conducted several tests of transpired solar collectors to determine the air volume that could be cooled at night, and the temperature drop from ambient was measured. The tests confirmed that nocturnal radiative cooling can cool ambient air by as much as 4.7 °C below the ambient value [89]. A patented air-based system that was composed of perforated metal panels was developed by Conserval Engineering (see Fig. 11), and it harnessed radiative cooling at nighttime and above the sheathing ventilation during the day [90]. An idea of regulated skylights for cooling purposes by radiative cooling was theoretically introduced by Falt et al., and the weather data in Helsinki was used to assess its performance [91].

Air-based systems are quite simple and are cheaper to install [20]. The radiators must have a narrow air channel and a large surface area to maximize the thermal contact with the air. Nevertheless, it is often the case that the cooling gains are limited compared to the fan power and that the systems have underperformed. Furthermore, the application of these systems to buildings is difficult to implement, and architectural integration is rather poor, because the systems can be adopted only in a detached house or the last floor of a duplex or multi-story building.

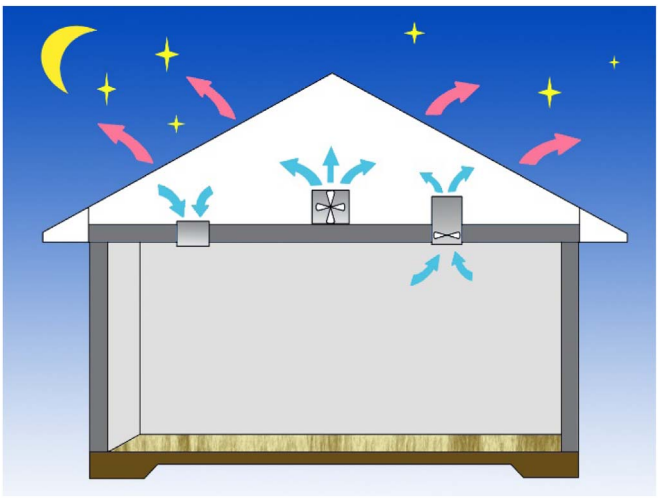

Fig. 10. Schematic diagram of the full-scale NightCool Concept [87].

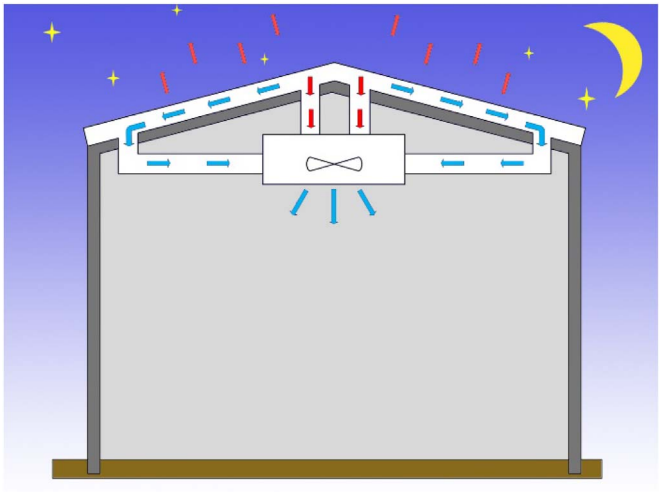

Fig. 11. Schematic of a patented air-based PRC system [90].

3.1.3. *Hybrid systems*

To better exploit the cooling resources, varieties of novel systems have been derived on the basis of using night radiator systems for heat pumping. A combination of nocturnal cooling and other energy-related systems is listed in Table 5 and described in the following section.

A photovoltaic-thermal (PVT) collector for cooling energy and power generation is one of the illustrations of hybrid systems [92]. Experimental and analytical studies of uncovered PVT collectors were conducted in Stuttgart. Large PVT modules were then developed and implemented in a ZEB (Zero Energy Building). These modules served the dual function of regenerating the phase change material (PCM) ceiling and cooling down the storage tank, which was used as a heat sink for a conventional chiller during the daytime. Similarly, a feasibility study of nighttime radiative cooling of an air-based building that integrated a photovoltaic-thermal (BIPVT) system under the climatic conditions of major Australian cities was presented by Sohel et al. [93]. Later, the same authors developed a novel ceiling ventilation system that was integrated with PVTs and PCMs in a Solar Decathlon house for operation during both winter and summer using daytime solar radiation and night-time sky radiative cooling, respectively [94]. In summer, the panels extract heat from the air that flows through the PVT by emitting radiation to the dome (see Fig. 12), which enables the outlet air to be 3 °C lower than the inlet air temperature [95].

As a promising thermal storage media, PCMs integrated with cooling panels could provide an alternative to effectively using the cooling resources because the nocturnal radiation is intermittent and has relatively low energy density. As mentioned earlier, the cold water produced at night is utilized to cool the PCM ceiling in the design of some passive and low-energy housings [92]. An integrated system that contains a micro-encapsulated phase change material (MPCM) slurry storage and a nocturnal sky radiator system was proposed by Zhang et al. and is supported with a

Table 5
The hybrid systems that utilize nocturnal radiators.

No.	Nocturnal radiative cooling coupled with / Served as	Reference work
1	Photovoltaic-thermal (PVT) collector	[92–95]
2	Phase change material (PCM ceiling/MPCM)	[92,96]
3	Evaporative cooling (DEC/IEC)	[97,98]
4	Heat pipe/Thermosiphon	[99–101]
5	Solar desiccant	[102,103]
6	Solar collector wall	[104]
7	Heat rejecter of cold source equipment	[105]

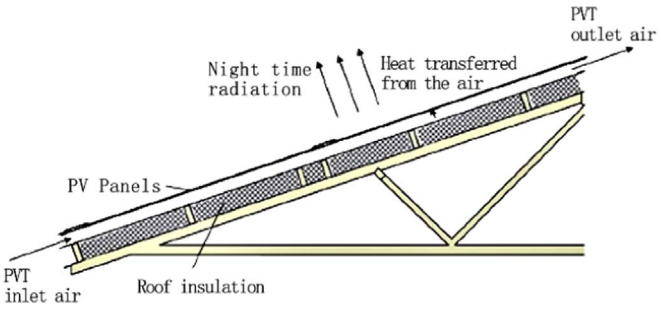

Fig. 12. Schematic diagram of night-time operation of the PVT module [94].

mechanical chiller and dedicated air handling unit [96]. In this study, the cold water storage is replaced by novel phase change material. The energy saving potentials of five typical cities across China are predicted with the maximum value of 77% in Lanzhou (semi-arid climate) and the minimum value of 11% in HongKong (humid climate).

Investigations on combining nocturnal cooling and evaporative cooling have also been performed. Heidarinejad et al. studied two types of evaporative cooling systems in Tehran: direct evaporative cooling (see Fig. 13(a)) [97] and indirect evaporative cooling (see Fig. 13(b)) [98]. At the first stage of two systems, the hot outdoor air was pre-cooled by the requisite cold water provided by nocturnal radiative cooling. Then, the pre-cooled air passed through a direct evaporative pad or an indirect evaporative cooler. The pre-cooling was a renewable and pollutant-free process, which augmented the efficacy of the two cooling systems.

A heat pipe or thermosiphon is a known and reliable passive technology that has been extensively used for heat transfer. The combination of nocturnal radiative panels and thermosyphon heat pipes was proposed and developed by different researchers. Ezekwe designed, constructed and tested the performance of a

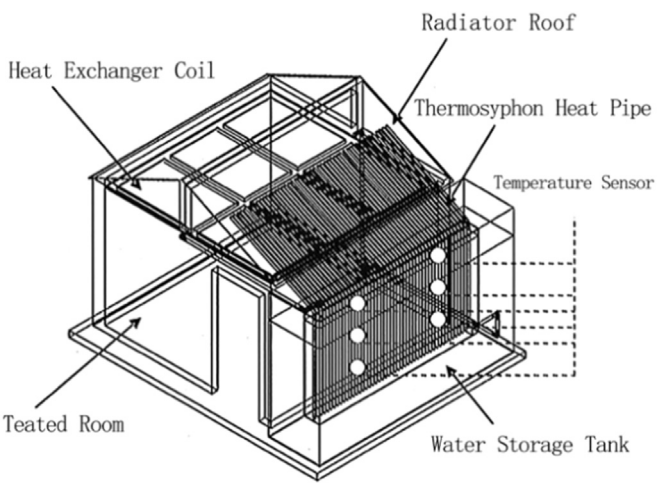

Fig. 14. Schematic diagram of a heat pipe-assisted nocturnal radiative system [100].

heat pipe-assisted night sky radiative cooler in Nigeria [99]. These experiments demonstrated that the system has a cooling capacity of 628 kJ/m^2 per night, and it attains the temperature of 12.8 °C in a cold chamber with an ambient temperature of 20 °C. A similar test of the thermosiphon heat pipe radiator was conducted in Chiang Mai, Thailand, with a theoretical model developed and verified by experimental results (see Fig. 14) [100]. The temperature in the room during the summer daytime could be reduced by approximately 4.0–5.0 °C from the ambient temperature. In a further study, the developed model was applied to seasonal analyses for Bangkok and Chiang Mai, Thailand, where the climates are hot and humid vs. hot and semi-humid, respectively, and for Alice Springs, Australia, where the climate is hot and semi-arid [101]. In

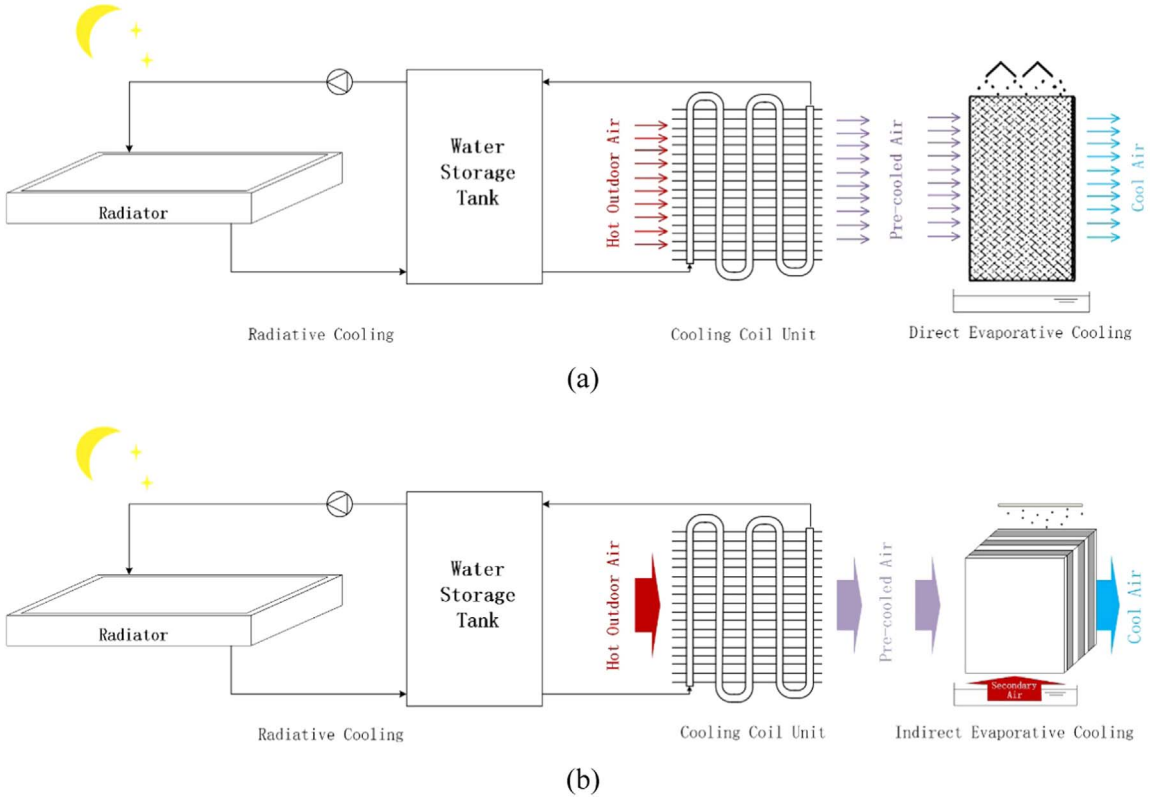

Fig. 13. Schematic diagram of a hybrid system that combines radiative cooling and (a) Direct Evaporative Cooling [97] and (b) Indirect Evaporative Cooling [98].

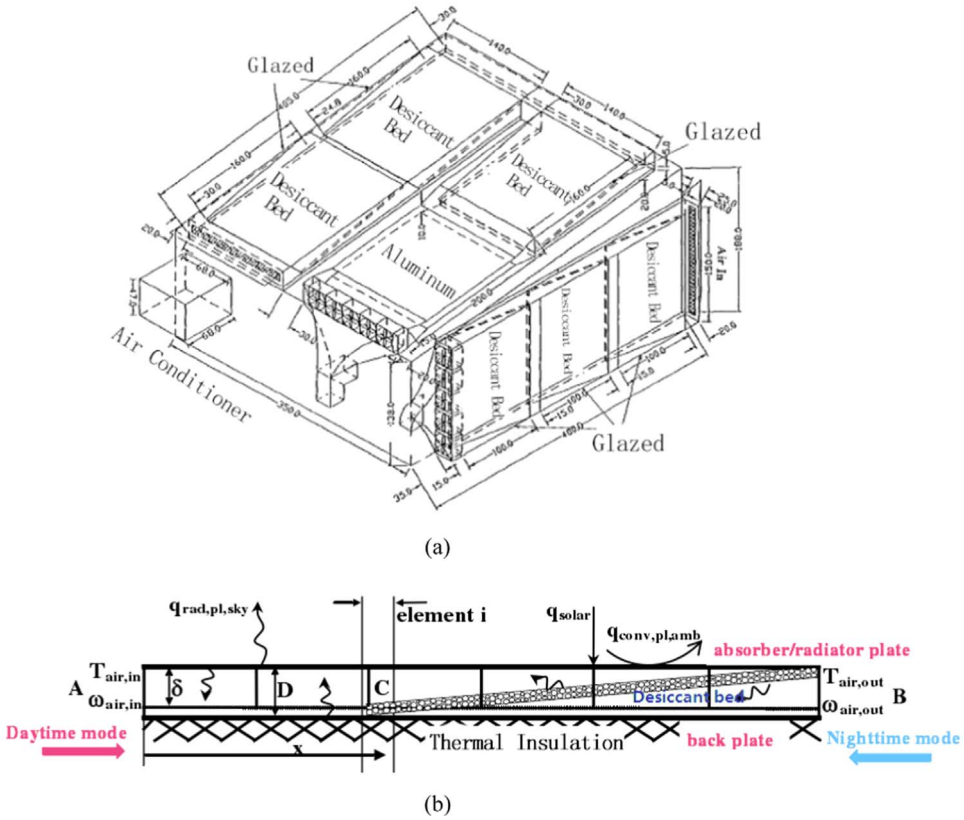

Fig. 15. Schematic of the desiccant nocturnal radiative cooling-solar collector system (a) in Lu's paper [102] and (b) in Ali's paper [103].

the simulation, Alice Springs showed the highest potential, followed by Chiang Mai and Bangkok.

The concept of a solar desiccant-enhanced radiative cooling (SDERC) system was introduced by Lu et al. [102]. As depicted in Fig. 15(a), a full-scale SDERC system with a conditioned house was set up and tested in Taiwan. Three independent subsystems were built on the upper roof and east and west sides of the house. The ambient air undergoes a dehumidification process at night and undergoes a regeneration process when exposed to sunlight. Because the isothermal desiccation process has a larger capacity for moisture absorption and operates at a lower temperature than an adiabatic process, the moisture removal capabilities of the desiccant materials and the heat rejection capabilities of the nocturnal sky radiation could complement each other. A design that is analogous to this configuration was presented by Ali in Egypt, as shown in Fig. 15(b) [103]. During the night, ambient air travels from location B to C and is dehumidified by the desiccant bed. The remainder of the radiator plate serves to cool the air stream without dehumidification. During the daytime, the ambient air travels from location A to C and is heated by the absorbed solar radiation. Then, the air stream regenerates the desiccant bed and is exhausted to the outside. A mathematical model for analyzing the heat and mass transfer during the adsorption and regeneration is established and was verified by Lu's experimental data. The model results demonstrate that this system is feasible for air comfort applications in hot arid areas such as Upper Egypt. The processed air is simulated to have a temperature that is lower by 5–7 °C compared with the ambient air, with a relative humidity that is not higher than 40%. The air can be drawn into the inner space for low humidity drying or air-conditioning purposes.

Another hybrid system in which nocturnal radiative cooling was coupled with a solar collector wall to produce a building-integrated solar heating and cooling panel (called SHCP) that served as construction components for a building roof or envelope was proposed by Cui et al. [104]. An experimental apparatus was established for detailed study of its performance. The experiment results show that in the extreme cold of January in Tianjin, China, the daily average heat-collecting efficiency was 39%, with a maximum of 65%, while during hot seasons, the average cooling capacity can reach 87 W/m^2.

Usually, building owners do not prefer to utilize cooling towers due to their appearance, land use, and water supply, as well as noise issues [105]. Hence, the nocturnal radiative cooling that serves as the supplemental heat sinks of the cold source is a possible alternative for buildings that do not have sufficient land area. Man et al. proposed a novel hybrid ground-coupled heat pump (HGCHP) system that has a nocturnal cooling radiator (NCR) [105]. A practical analytical model of the novel system is built to simulate the system operation performance. Systems with different configurations are designed and simulated for the sample building in HongKong. The results indicate that the system is feasible to use when the nocturnal radiative cooling is used as a supplemental heat rejecter for cooling load-dominated buildings, even in humid subtropical climate areas, and it can save 10.22% of the total costs during 10 years of operation.

Many synergies of nocturnal radiative cooling with other energy-related technologies in buildings have been tapped. However, the majority of the hybrid systems are still at the early experimental or prototype testing stages. Data on field applications are scarce, and experimental data require robust models to predict the amount of heat that is dissipated by the systems.

3.2. Daytime cooling

PRC is universally acknowledged to perform better at nighttime, while the peak cooling load of buildings occurs in the daytime. Daytime radiative cooling under direct sunlight is difficult because the outgoing radiation is offset and overtaken by the

incoming solar radiation. To reduce the cooling load of a building during the day, cool roof ideas have led to the development of radiative tiles or coatings, which have high reflectance plus high emissivity, as discussed in Section 3.2.1. Section 3.2.2 describes the progress in research on selective surfaces under solar irradiance, which could facilitate the realization of daytime cooling.

3.2.1. Cool roofs

Cool coatings are often applied on roofs, which is typically referred to as 'cool roofs' [106]. Reflectivity (or albedo) α, Emissivity E, and R-values are the three dictating material factors on the overall performance of a cool roof. By emitting off the stored heat in an opaque material under a clear sky and reflecting off incoming solar radiation during the daytime [107], cool roofs render the external surface colder, reducing the cooling demands of buildings and easing the urban heat island phenomenon for pumping the heat to outer space [108,109]. In addition, raising the roof R-values can also reduce the daytime heat gains, but at the cost of nighttime heat losses. Gentle et al. studied the three parameters in combination (α, E, R) and determined that $R \leq 1.63$ plus high α and high E is the preferred option for cooling with respect to the cooling demands and initial cost benefits [110]. Aubrey held a similar opinion and stated that the solar reflectivity is the primary determinant of the cool-roof performance [111]. However, for most cool roofs in current use, solar reflectivity is not high enough to consider a lowering of E, which allows a faster rate of cooling for realistic total heat inputs [58].

Recent developments from the photonics and optics world could be leveraged to improve cool roofs, which uses nanotechnology to increase both the solar reflectance and infrared emittance of the roof [112]. Combining a high solar reflectance and high IR absorptance in a single material requires a large spectral switch near 2.5 μm and is quite practical with certain select paints and some vacuum and chemically coated systems [110]. For example, the use of aluminum flakes that are precoated with nanothin SiO_2 layers via a sol-gel coating before an iron oxide layer is applied [5]. Sheet glass without iron content is also suggested as a practical material that has high reflectance and a large radiation output. In another report, Gentle et al. proposed a 'supercool roof' using birefringent coated polymer stack and achieved an appealing result of 2 °C below the ambient temperature under a direct 1060 W/m^2 direct sunshine [113]. Besides, a novel radiative roof coating that allows us to curb unwanted heat gains during the diurnal cycle was presented by Muselli, and the simulation of their prototype demonstrates that the cooling energy consumption can be reduced by 26–49% [114]. Despite the fact that heating gains are reduced throughout the daytime in the summer, heating penalties in winter should be considered when designing a cool roof because the heating-dominated buildings may not be suitable [115,116].

3.2.2. Selective phontonic cooling apparatus

In the pursuit of net cooling during the daytime, researchers have experimented with thin selective films under direct sunlight [54,117–121]. However, most approaches have proven to be insufficient for fulfilling the purpose of an ideal daytime thermal emitter. Recently, an ingenious photonic radiative cooler was proposed to passively lower the temperature of the radiator surface under direct sunlight. Using a thermal nanophotonic approach, it is composed of an integrated nanophotonic solar reflector and a thermal emitter, and it reflects 97% of the incident sunlight while emitting strongly and selectively in the atmospheric transparency window [54]. When exposed to direct solar irradiance of 850 W/m^2 on a rooftop, the nanophotonic radiative cooler has a cooling power of 40.1 W/m^2 at the ambient temperature. These results indicate that a tailored nanophotonic approach can provide new technological possibilities for energy efficiency, and the cold darkness of the universe can be used as a renewable thermodynamic resource even during the daytime. However, the results presented are given under certain conditions. The exact cooling magnitude in different regions and climates should be known to better utilize this ground-breaking technique. In the next section, the cooling potential of the PRC will be discussed in detail.

4. Cooling potential and applications prospects of PRC in buildings

The following section details the cooling potential and application prospects of passive radiative cooling in buildings. In Section 4.1, the cooling potentials of both nighttime and daytime radiative cooling are evaluated. Section 4.2 provides a discussion on the application challenges and prospects.

4.1. Cooling potential assessment

In this section, the nocturnal and daytime cooling potential of various system configurations in different geographic zones are reviewed and assessed to offer insights for researchers who are continuing the quest.

4.1.1. Discussion on nocturnal radiative cooling potential

Atmospheric conditions have a significant impact on the cooling potential of nocturnal PRC systems. The regional expansion of the nocturnal PRC system application is summarized in Fig. 16 from core journal and conference papers, where the number in the circle represents studies on nocturnal PRC systems that have been conducted in each country. Fig. 16 shows that the nocturnal PRC systems are widely distributed in most middle and high latitude regions, especially some Mediterranean circumjacent countries.

Table 6 details the above reviewed papers mainly on the issues of the cooling potential. The study year, location, system configuration and research method (experiment, simulation or field test) are tabulated. The cooling potential of the nocturnal PRC is characterized by the maximum or average cooling power density, the temperature depression of the air temperature, and the water or surface temperature.

Table 6 and Fig. 16 show that the studies on the nocturnal PRC hitherto have been very mature and extensive, combining many other systems to achieve cooling. The nocturnal PRC is well adaptable in temperate and Mediterranean climates with larger diurnal temperature swings, lower humidity and minimal cloud covers. In Table 6, the findings that have cooling power density in excess of 70 W/m^2 were often conducted in the fall or winter under favorable atmospheric conditions, and the convective heat transfer reinforces the net radiative power. In other cases, the high cooling power density is derived from studies of selective surfaces, for which the results are computed, and most have not been used in experimental applications.

Most regions can provide net nocturnal radiation of 30–40 W/m^2, at the same time achieving the functions of each system (e.g., cooling air, water). Under favorable conditions, an air-based system can lower the inlet air temperature by 2–4 °C, while a water-based system can achieve an average 3 °C temperature depression with a large water flow. The comparatively low cooling power density, the fact that the peak cooling load occurs in the daytime and the limited roof area are major hurdles in commercializing the nocturnal PRC in buildings because the cooling load of a commercial building reaches at least 100 W/m^2. In other words, it will be a large leap if we achieve daytime cooling in buildings by attaining a large cooling magnitude.

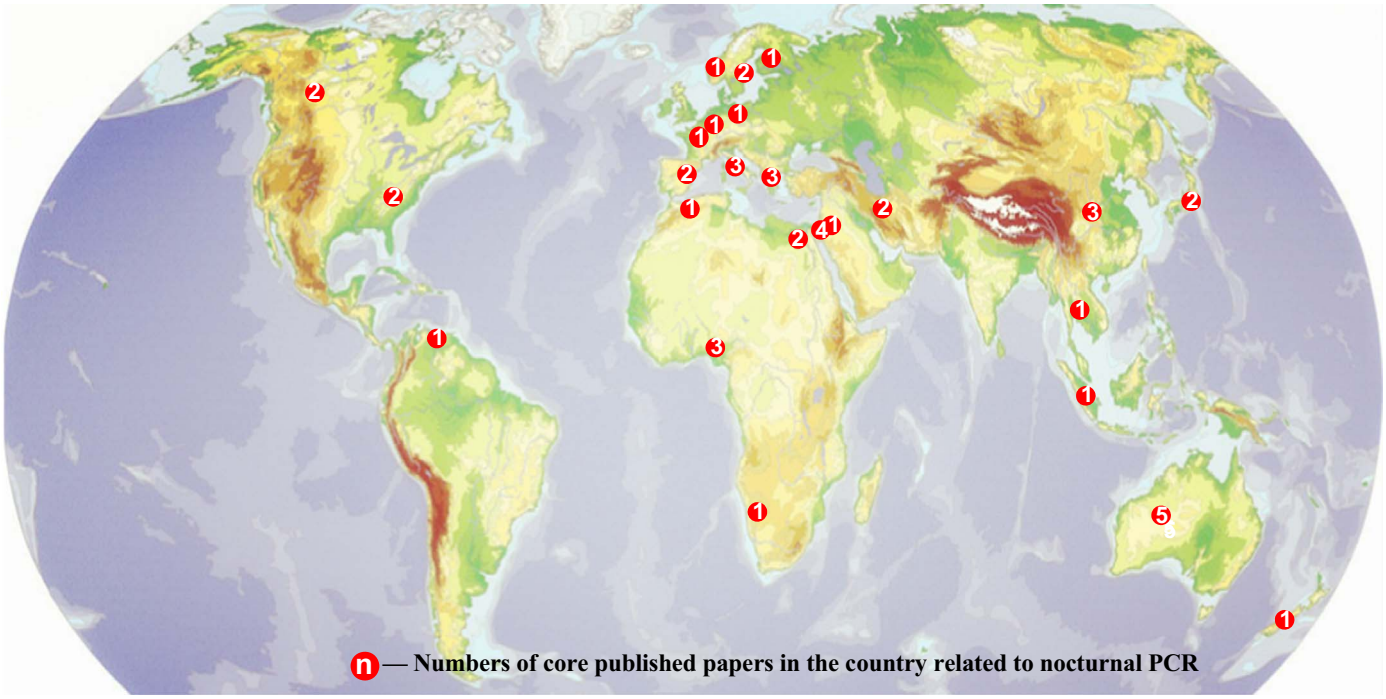

Fig. 16. Cartogram of the core published papers related to nocturnal PRC, in different countries.

4.1.2. Estimation of the diurnal radiative cooling potential

There is no denying that the research by Raman et al. [54] is path-breaking and worthwhile, but it still leaves a substantial amount of room for thought. The results are given for a clear, sunny winter day when the daytime ambient temperature is approximately 20 °C, in the dry California air. However, the experimental results are not sufficient to address the fact that the maximum temperature depression of the surface reaches only 4.9 °C, over all costs of cooling power density at the best times. The experimental results are carefully validated by a reliable theoretical model, but in this paper, the simulated models under atmospheric conditions across different geographical regions are not presented. Because the applications prospects and the development of emerging techniques are closely associated with the cooling magnitude and the surface temperature, a model reproduction is shown in this section to assess the daytime radiative cooling potential.

Based on the calculation method discussed in Section 2, we model the potential of the daytime cooling in the mid-latitude region as represented by Shanghai and the tropical region as represented by Bangkok in the summer and winter daytimes. In the calculation process, we solve Eq. (1) for the surface temperature using a binary search. Specifically, we input absorption/emission data on the surface that was obtained from the paper by Raman et al. [54], with the solar spectrum weighted to the net irradiance and the ambient temperature at a ten-minute interval. The atmospheric transmittance is modeled by PCModwin at different atmospheric modes and water vapor content. A 5% uncertainty is assigned to arise from the atmospheric modeling [54]. The heat transfer coefficient is assumed to be 4–6.9 W/(m^2 K) according to the paper by Raman et al. Fig. 17 shows the maximum temperature depression of the model in the mid-latitude region (Shanghai) in winter. The result shows that the maximum temperature depression can reach up to 4.7 °C under direct sunshine when h_c equals 6.9 W/m^2, which is basically in accordance with the result by Raman et al. When h_c decreases to 4 W/m^2, the temperature depression during the daytime increases by up to 7.0 °C. By hindering the convection heat transfer, the cooling effect of the surface enhances remarkably in winter in the mid-latitude region. However, the majority of the cooling demand occurs in the summer daytime, and hence, it makes more sense to determine the cooling capacity in the summer daytime.

The summer in the mid-latitude region (represented by Shanghai) and tropical region (represented by Bangkok) are modeled using a similar method, and the atmospheric conditions settings are both desired to be without aerosols, clouds or rain, as presented in Fig. 18 (a) and (b). When h_c equals 6.9 W/m^2, the maximum temperature depression accounts for 2.3 °C and 0.1 °C under direct solar radiation in Shanghai and Bangkok, respectively. Thus, it can be observed that the cooling magnitude of the daytime PRC is relatively poor in the mid-latitudes and would be expected to be worse in the hot and damp tropic zones. The measures that were taken to inhibit the convective losses had little impact on the decreases in the surface temperatures. The poor performance of the daytime PRC in summer inevitably constrains the application of the technique.

Because there is a trade-off between the cooling power density and the surface temperature depression, to determine the surface temperature at different cooling powers, a hypothetical electric heater is attached to the underside of the surface to demonstrate the variation in the surface temperature depression in the Shanghai summer. The stepped ascending heat input is applied constantly for 30 min, and the surface temperature rises and plateaus. Fig. 19(a) shows the surface temperature variation for the corresponding heat input under a steady state, and Fig. 19 (b) depicts the correlation between the temperature depression and the cooling power magnitude. The temperature reaches an ambient temperature with an input heating power of 20.1 W/m^2, and the maximum temperature depression equals 2.3 °C, which indicates that the cooling magnitude is not impressive from this device in summer.

From the model reproduction discussed above, it is quite clear that the cooling potential in the summer daytime is rather modest in different geographic regions, which limits the application of the new-type radiative cooler. The odds of low-temperature water production by this device in summer are very slim for the small surface temperature depression and the corresponding cooling

Table 6
Summary of the cooling potential of nocturnal PRC systems, in core papers.

Ref.	Year	Country	System configuration	Experiment	Simulation/ Calculation	Cooling Power/Temperature Depression
[122]	1978	Australia	Air-based Radiator	√		29 W/m^2 (278 K)
[84]	1998	Italy	Air-based radiator		√	Maximum 55.6 W/m^2 (clear day); 44.9/m^2 (cloudy day)
[73]	1988	Israel	Air-based radiator	√		t_{air} drop: maximum 7.2 °C
[75]	1993	Greece	Air-based Radiator		√	t_{air} drop: maximum 4 °C
[86]	1999	Thailand	Four air-based radiators	√		t_{air} drop:1–6 °C
[85]	2007	Greece	Air-based radiators	√	√	t_{air} drop: average 6 °C
[88]	2007	US	NightCool System (Air-based)	√		Average 5–10 W/m^2
[89]	2010	Canada	Air-based transpired radiators		√	t_{air} drop: maximum 4.7 °C
[82]	2014	Spain	Three Radiators with different ε_e	√	√	63.7,42.2,7.5 W/m^2, respectively
[118]	1975	Italy	Selective radiator	√	√	Maximum 52 W/m^2 (Ex), 60 W/m^2 (Simu); t_{sur} drop: maximum 11 °C
[123]	1977	Italy	Selective radiator	√	√	Maximum 57 W/m^2 (Ex), 59 W/m^2 (Simu); t_{sur} drop: maximum 9 °C
[124]	1977	Canada	Selective radiator (TiO_2)	√	√	t_{sur} drop: maximum 15 °C
[25]	1980	Sweden	Selective radiator (SiO_2)	√	√	Calculating maximum 61 W/m^2; 32.5 W/m2 (298 K)
[125]	1985	Sweden	Selective radiator (Si_3N_4)	√	√	63.8 W/m2 (298 K);48.8 W/m2 (293 K)
[126]	1995	Belgium	Selective radiator (SiO_xN_y)	√	√	61.8 W/m^2 (298 K); 46.4 W/m^2(293 K)
[127]	1984	US	Selective radiator	√	√	50–75 W/m^2
[21]	2015	Australia	Selective radiator (CMM)	√		Maximum 116 W/m^2
[3]	1995	Egypt	Water-based Radiator	√	√	Maximum 54 W/m^2; Average 33 W/m^2; t_{water} drop: average 8.3 °C
[128]	1986	Nigeria	Water-based radiator	√		Average 70 W/m^2
[129]	1989	Japan	Water-based radiator	√		Average 50 W/m^2; t_{water} drop: 2–5 °C
[76]	1996	Jordan	Water-based Radiator(Mild Steel)	√	√	t_{water} drop: maximum 5 °C
[78]	1999	Israel	Water-based radiator (Polypropylene)	√	√	Maximum 91.4 W/m^2
[52]	1999	Norway	Water-based radiator (PPO resin)	√	√	Maximum 60 W/m^2
[51]	2000	Israel	Water-based radiator	√	√	t_{water} drop: maximum 3.2 °C
[130]	2005	Namibia	Water-based Radiator(Mild Steel)	√	√	Average 60.8 W/m^2
[50]	2006	Greece	Water-based radiator (Integrated with building envelope)	√	√	Average 55.9 W/m^2 (Exper); t_{water} drop: maximum 6.5 °C
[26]	2007	Australia	Water-based radiator	√		55 W/m^2 at $t_{ambient}$
[81]	2011	Nigeria	Water-based radiator	√	√	Average 66.1 W/m^2
[79]	2012	Iran	Water-based radiator (Galvanized iron)	√	√	Average 45 W/m^2; t_{water} drop: maximum 7 °C
[80]	2013	NewZealand	Water-based radiator	√	√	Average 50 W/m^2
[131]	1992	Israel	Roof pond	√		Average 17 W/m^2
[132]	2000	Venezuela	Roof pond	√		19–24 W/m^2
[91]	2011	Finland	Skylight		√	Average 4 W/m^2
[133]	2012	Australia	NPRC+ water spraying system		√	Maximum 105 W/m^2
[103]	2013	Egypt	Desiccant enhanced radiator		√	75–85 W/m^2
[97]	2008	Iran	NPRC+ Direct evaporation	√	√	t_{air} drop: Average 8 °C
[98]	2010	Iran	NPRC+ Indirect evaporation	√	√	t_{air} drop: Average 10 °C
[96]	2010	China	NPRC+MPCM		√	Average 111 W/m^2
[92]	2007	Spain	NPRC++PVT	√	√	43–62 W/m^2 at T_{tank}=20.9 °C
[99]	1988	Nigeria	Heat pipe radiator	√	√	Average 15 W/m^2; t_{air} drop from 20 °C to 12.8 °C
[104]	2015	China	Solar heating and cooling panel (termed as SHCP)	√		Maximum 85 W/m^2
[27]	2009	Australia	Radiator with aperture geometry		√	Maximum 135 W/m^2; t_{sur} drop: maximum 10 °C below ambient.
[134]	2000	Japan	Transparent polyethylene film coated with an aluminum layer	Field test		40–60 W/m^2

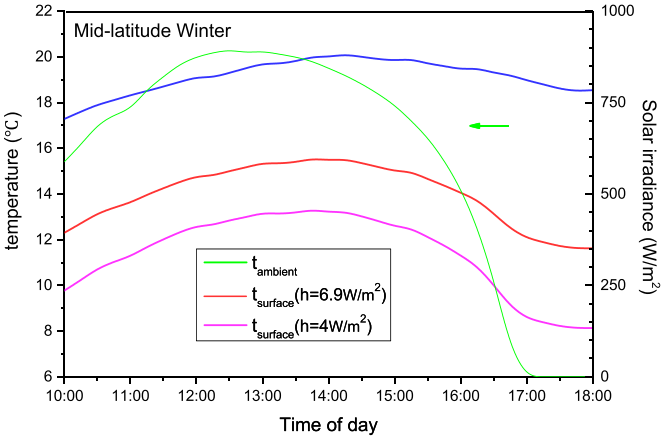

Fig. 17. The temperature variation of the ambient air and surface (h_c=6.9 and 4 W/m^2) in the mid-latitude region in winter.

power. The multilayer surface could be used to reduce the cooling load of a building on a summer day, such as acting as cool roof material, but the duration and corrosion resistance are still unknown. The complex production process and high cost of the new-type multi-layer surface by the thermal photonic approach are also obstacles to the development of daytime cooling in the summer.

The chart depicted in Fig. 20 illustrates the power magnitude of each constituent part of Eq. (1) at the intersection point of A and B, as marked in Fig. 19. It can be observed that the incoming power from the atmosphere accounts for a large proportion and has minor changes during a typical day. The convective heat gains also become a considerable part, which cannot be overlooked in pursuit of a low surface temperature. The special configuration reviewed in Section 2 could help to reduce the radiative heat gain, but the net effect is ambiguous.

To summarize, the new-type photonic material can achieve a desired cooling effect only on a mid-latitude clear winter day; however, under slightly unfavorable conditions, it has little cooling

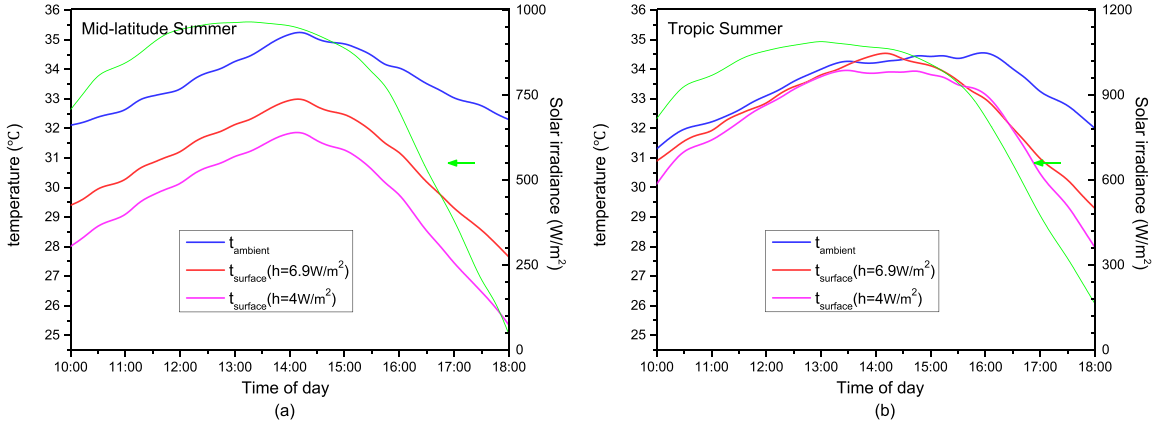

Fig. 18. The temperature variation of the ambient air and surface (h_c=6.9 and 4 W/m^2) in summer (a) in the mid-latitude zone (Shanghai) and (b) in the tropic zone (Bangkok).

potential according to its optical properties, which impedes the specific implementation and integration of the radiative cooler with other HVAC systems.

4.2. Challenges and prospects

In this section, we highlight the barriers that likely exist to widespread commercialization as well as scopes for further development of passive radiative cooling in buildings.

4.2.1. Technical problems

Advances in composite materials with radiative cooling potentials have opened a new window to achieve the ability to operate in the daytime and reach temperature below the ambient temperature. However, they have a relatively modest performance in the peak cooling period as stated in Section 4.1 mainly due to their inability to meet the strict spectral emittance of the ideal selective coating. For the photonic nanostructures by tailored Raman et al., the IR emission is not strictly selective and the emission within the atmospheric windows is not very strong [54]. For the microstructure photonic devices, they need to be combined with solar reflectors to avoid substantial solar radiation, thereby destroying the strictly selective IR emission [21]. Meanwhile, there are significant manufacturing and scale-up challenges because

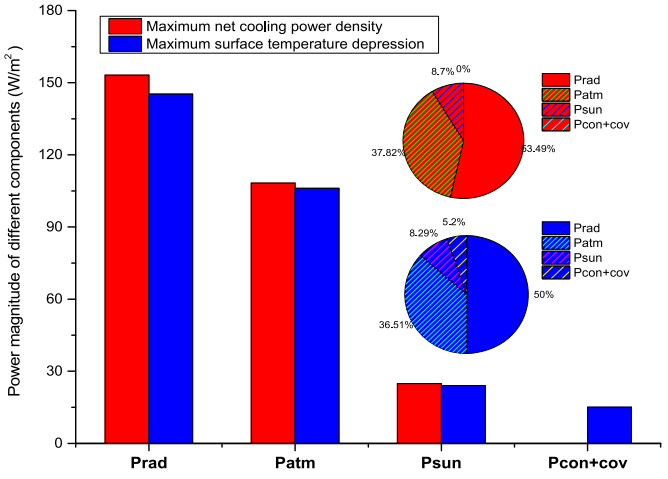

Fig. 20. Power magnitude of different components under the A and B conditions.

they are still in early research and development. Additionally, the maintenance and incorporation into the building infrastructure are also big challenges. Hence, the possibility of achieving a desired cooling effect during the daytime is mainly accounted for by the material itself, and fabricating a material that approaches the

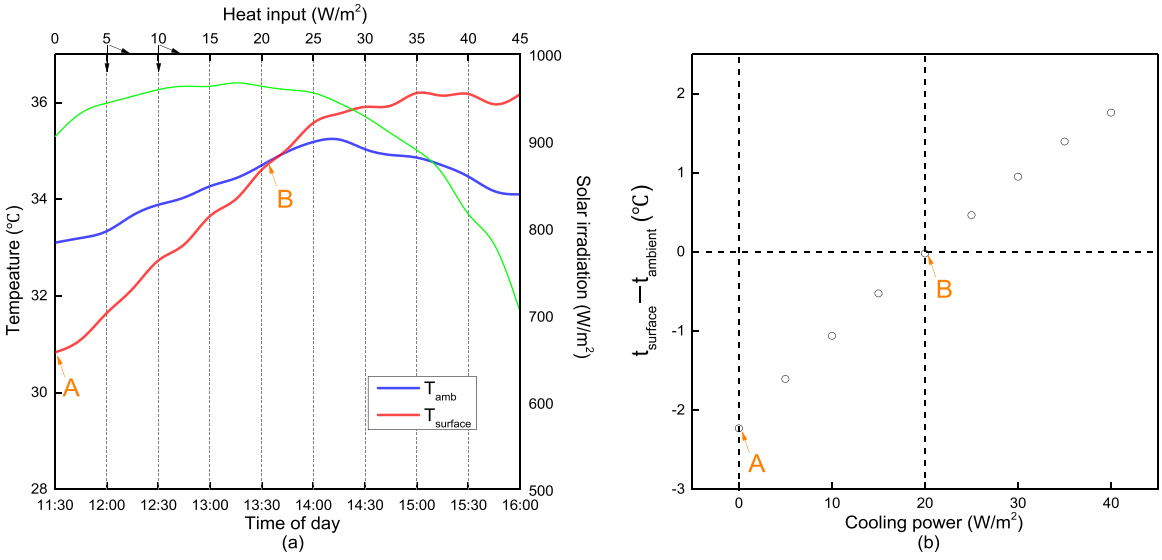

Fig. 19. (a) The surface temperature variation for the corresponding heat input at each step under steady state. (b) The correlation between the cooling power and surface temperature depression.

properties of an ideal selective material is still in the future. However, deterministically manipulating thermal emittance at certain wavelengths while increasing solar reflectance prevents new possibilities for us. In addition, nonreciprocal materials that could violate Kirchhoff's law can achieve a difference between directional spectral emissivity and absorptivity by the control of thermal radiation, which could offer a new insight toward achieving substantial daytime cooling [135].

Another technical problems arises from the spatial concerns. Radiative cooling to satisfy a substantial fraction of building cooling loads requires an inherently large areas. The roof ought to be horizontal or moderately pitched if the cooling panels are to be integrated with it to ensure their full exposure to the sky. For these reasons, this technology cannot meet the cooling requirements of multi-storey buildings where the ratio of roof area to floor area is small. Therefore, small- and medium-sized shorter buildings are the targets of the proposed technology.

There exist other technical problems such as parasitic energy losses in every heat transfer process (e.g., energy losses in the water storage tank and between the radiative surface and the heat transfer fluid), complex and holistic design of the PRC systems, etc. Due to the intricacy of the PRC, it is generally infeasible for retrofits and hard for building operations and maintenance staffs (O&M) to understand and manage the system and its components [136].

4.2.2. Geographic constraints

The geographical conditions play a pivotal role in practical applications of PRC systems in buildings. Some of these are the atmospheric constituents (i.e $\cdot H_2O$, CO_2), sky condition (i.e. overcast vs. clear), wind speed and condensation situation. The knowledge of the metrological conditions and the applicability (i.e. the level of expected savings) of any locations are necessary to be addressed before embarking on PRC.

As stated in Section 2.1.3, the water vapor content mainly contributes for the atmospheric radiation within the 8- to 13-micron window. Hossain et al. [137] investigated the effect of humidity on the radiative cooling performance by estimating the cooling potential for variable relative humidity (RH) in two mid-latitude locations in Australia. They concluded that the atmospheric water vapor on system efficiency can be significant, especially for selective radiators. In addition, the atmosphere will be utterly opaque to IR radiation for an overcast sky and any effective cooling will not be possible [137]. Hence, the PRC techniques are most adaptable in areas with lower humidity and minimal cloud covers. Pacific Northwest National Laboratory lists the locations that may limit the impact of radiative cooling with the following summer characteristics [136]:

- Locations where the majority of summer nocturnal hours are very warm (above 27 °C).
- Locations where the majority of summer nocturnal hours are hot and humid (above 80% RH, with temperatures over 24 °C).
- Locations with frequent hot summer days and very short summer nights.
- Small buildings in marine climate with low cooling loads.

Though atmospheric radiation accounts for a large proportion of incoming flux, technical approaches of blocking it to a radiator fully open to the sky are suggested in Section 2.1.2 by using heat mirrors or apertures with confining radiation to the sky into a small solid angle, which prevents the incoming atmospheric radiation from large zenith angles.

4.2.3. Cost issues

Generally, PRC systems carry their own significant installation costs; however, these costs can be mitigated by the potential to eliminate ductwork, eliminate plenum spaces between floors (potentially shortening the building height), and significantly downsize or eliminate key HVAC components such as chiller. Furthermore, cost savings accompany related energy savings and electricity cost savings from free cooling will be realized every year the system runs. Whether energy savings justify the large initial costs, this section discusses the cost-saving potentials of utilizing PRC systems in terms of different system configurations: cool roofs, conventional radiators and photonic radiators.

Currently, there are not many commercial radiative cooling systems that can be readily installed for building space cooling. Cool roofs are one of the typical examples for the commercialization of PRC in buildings. Levinson et al. estimated prototype energy saving and heating penalty per unit conditioned roof area and concluded that retrofitting 80% of the 2.58 billion square meters of commercial building conditioned roof area in the USA would yield an annual energy cost saving of $735 million [138]. For cool roofs working in cold climate, Hossein used DOE-2.1E and shown that a cool roof could save in annual overall energy expenditure up to about $60/100 m^2 of the roof area for a retail store building in Anchorage and Montreal [139].

For the conventional radiator systems, several components are expected to carry significant first costs, including the rooftop radiator, radiant cooling panels, thermal storage tanks, insulation and connection pipes. A system combining a water radiator linked to a cooling panel experimented at the Athen Renewable Energy Sources was reported to cost 116 Euro/m^2 (Cost figures for late-1990s) [140]. Two novel radiators (called Heliocoil and Polycarbonate) tested in Sde-Boqer cost 60 and 50 Euro/m^2 respectively [140] (Both cost figures for late-1990s Euro). A field test of a closed water-based radiative system was conducted in New Mexico and the economic analysis demonstrated that the payback period for the closed system was calculated to be approximately 6.8 years [141]. Compared to covering a large fraction of the roof with radiators and using tubing to flow water, rooftop spray-cooling systems are popular in commercialized technologies due to the low cost involved. The WhiteCap roof system was reported to have an installation cost for the rooftop spray system of $400 per 1000 ft^2 of roof surface (In 1998 U.S. dollars) [142]. The additional cost of the NightSky system in Vacaville, CA was $14.53/$m^2$ of building floor area (Late-1990s U.S. dollars) [143].

For the novel photonic systems, the technology is still at the laboratory prototype stage and the cost of the photonic products at production scale are not known at this time. Pacific Northwest National Laboratory conducted the simulation to assess the cost benefits of the photonic radiative systems compared to several reference systems: VAV systems, custom radiators with high-end and median surface properties [136]. The report revealed that the novel radiative system saves 24–103 MWh electricity in five US cities compared to the benchmark VAV systems. It was also noted that to achieve a 5-year payback period, the maximum acceptable incremental cost for upgrading from nighttime cooling to photonic radiative cooling should range from $8.25 to $11.50/$m^2$ [136].

From the above discussion, it can be found that the applications of PRC systems in buildings are still in the immature stage and the energy savings may not justify the large initial costs due to the modest cooling potential. The cost-saving potentials are mostly indebted to the mass-production and optical property improvement of the novel material.

5. Conclusions

The current state-of-the-art of the literature on passive radiative cooling in buildings is presented. The salient points drawn from the study are as follows:

- The calculation models of PRC can be categorized into the selective dependent and selective independent model. Masses of empirical simplified models of the longwave radiation have been developed. All the integral models can be rendered into the generic biquadratic forms of the temperature, which are lumped in the emissivity and the equivalent sky temperature.
- The optimizing strategies to enlarge the net radiative cooling effect are analyzed from the basic physical models. For radiating out more heat, it is essential to select the appropriate existing radiative surfaces according to the cooling purpose. High emittance radiative surfaces are preferred for high thermal load cooling, while selective emitters prove to be more suitable for sub ambient cooling.
- Atmospheric radiation that is often hard to cut accounts for a large portion of the incoming heat gains. For reducing the atmospheric radiation, heat mirror apertures or angular selective surfaces can be employed.
- To suppress the convective terms, wind shields or different types of wind covers should be installed. The trade-off for less outgoing radiation and durability of the covers must be considered when designing and fabricating the radiative apparatus.
- Nocturnal PRC is an age-old practice that has been investigated extensively. The experimental and theoretical analyses have been conducted on the various systems such as roof ponds, air-based, or water-based systems. Combinations with other systems are also explored to maximize the cooling performance. PCM, MPCM, direct and indirect evaporative cooling, heat pipe and desiccant systems were integrated with the nocturnal PRC.
- Higher surface temperatures must compensate for the higher cooling power magnitude. The cooling magnitude of nocturnal PRC experimentation is usually maintained at 30–40 W/m^2 for distinctive cooling purposes; this amount is relatively modest, which hinders the commercialization of nocturnal PRC.
- The geographic factors, which include meteorological conditions and building locations, are necessary to consider. The most suitable locations for adopting nocturnal PRC are in temperate and Mediterranean climates, which have larger diurnal temperature swings, lower humidity and minimal cloud cover, as reflected by the distribution of the existing studies and applications of PRC.
- Daytime PRC is an emerging free-energy technique of great significance; if well performed, it can relieve conventional mechanical cooling and ease the burden on the grid at peak times. However, the cooling potential of daytime PRC is still restricted by the radiative surface material. As simulated, daytime PRC can hitherto be achieved under direct sun radiation on a clear winter day in the mid- and high-latitude regions. It is not likely to be implemented in periods and locations where daytime cooling is needed the most.
- Currently, the cooling magnitude, product reliability, coating optical properties, cover durability and building integration are the major inextricable obstacles. The wide application of PRC systems will strongly rely on the development of novel optical materials that better approach the ideal emitter or are indebted to nonreciprocal materials in which directional and spectral emissivity and absorptivity are not equal.

References

[1] Heier J, Bales C, Martin V. Combining thermal energy storage with buildings – a review. Renew Sustain Energy Rev 2015;42:1305–25.
[2] Omer AM. Energy, environment and sustainable development. Renew Sustain Energy Rev 2008;12(9):2265–300.
[3] Ali AHH, Taha IMS, Ismail IM. Cooling of water flowing through a night sky radiator. Sol Energy 1995;55(4):235–53.
[4] Daniel B, Irina M, Vadim N, Mark M, Jacques M. Using radiative cooling to condense atmospheric vapor: a study to improve water yield. J Hydrol 2003;276:1–11.
[5] Granqvist CG, Smith GB. Green nanotechnology: solutions for sustainability and energy in the built environment. CRC Press; 2010 ISBN-13:9781420085327.
[6] Zhu LX, Raman A, Wang KXZ, Abou Anoma M, Fan SH. Radiative cooling for solar cells. In: Proceedings of physics simulation and photonic engineering of photovoltaic devices Iv 2015; 9358.
[7] Bainbridge David A, Haggard Kenneth L. Passive solar architecture: heating, cooling, ventilation, daylighting, and more using natural flows Burlington: Chelsea Green Pub; 2011 ISBN-13: 9781603582964.
[8] Abrams Donald W. Low-energy cooling: a guide to the practical application of passive cooling and cooling energy conservation measures. Van Nostrand Reinhold; 1986 ISBN-10: 0442209517.
[9] Bowen A, Clark E, Labs K. Passive cooling. American Section of the International Solar Energy Society 1981. ISBN-10: 0895530333.
[10] Trombe F. Perspectives sur l'utilisation des rayonnements solaires et terrestres dans certaines regions du monde. Rev Gen Therm 1967;6(70):1285–314.
[11] Rephaeli E, Raman A, Fan S. Ultrabroad band photonic structures to achieve high-performance daytime radiative cooling. Nano Lett 2013;13(4):1457–61.
[12] Samuel DGL, Nagendra SMS, Maiya MP. Passive alternatives to mechanical air conditioning of building. A review. Build Environ 2013;66(4):54–64.
[13] Hughes BR, Chaudhry HN, Ghani SA. A review of sustainable cooling technologies in buildings. Renew Sustain Energy Rev 2011;15(6):3112–20.
[14] Chan HY, Riffat SB, Zhu J. Review of passive solar heating and cooling technologies. Renew Sustain Energy Rev 2010;14(2):781–9.
[15] Santamouris M. Passive cooling – the state of the art. Advances in solar energy.London: James And James Science Publishers; 2006.
[16] Pacheco R, Ordóñez J, Martínez G. Energy efficient design of building: a review. Renew Sustain Energy Rev 2012;16(6):3559–73.
[17] Sadineni SB, Madala S, Boehm RF. Passive building energy savings: a review of building envelope components. Renew Sustain Energy Rev 2011;15(8):3617–31.
[18] Ming T, Richter R, Liu W, Caillol S. Fighting global warming by climate engineering: Is the Earth radiation management and the solar radiation management any option for fighting climate change. Renew Sustain Energy Rev 2014;31:792–834.
[19] Hanif M, Mahlia TMI, Zare A, Saksahdan TJ, Metselaar HSC. Potential energy savings by radiative cooling system for a building in tropical climate. Renew Sustain Energy Rev 2014;32(5):642–50.
[20] Nwaigwe KN, Okoronkwo CA, Ogueke NV. Review of nocturnal cooling systems. Int J Energy Clean Environ 2010;11:117–43.
[21] Hossain MM, Jia B, Gu M. A metamaterial emitter for highly efficient radiative cooling. Adv Opt Mater 2015;3(8):1047–51.
[22] Gentle AR, Smith GB. Radiative heat pumping from the earth using surface phonon resonant nanoparticles. Nano Lett 2010;10(2):373–9.
[23] Bell EE, Eisner L, Young J, Oetjen RA. Spectral radiance of sky and terrain at wavelengths between 1 and 20 μm, II. Sky measurements. J Opt Soc Am A 1960;50(12):1313–20.
[24] Lushiku EM, Hjortsberg A, Granqvist CG. Radiative cooling with selectively infrared emitting ammonia gas. Appl Phys 1982;53:5526–30.
[25] Granqvist CG, Hjortsberg A. Radiative cooling to low temperatures: general considerations and application to selectively emitting SiO films. J Appl Phys 1981;52:4205–20.
[26] Gentle AR, Smith GB. Performance comparisons of sky window spectral selective and high emittance radiant cooling systems under varying atmospheric conditions.Sydney: Australian Solar Energy Society; 2011.
[27] Gentle AR, Smith GB. Angular selectivity: impact on optimized coatings for night sky radiative cooling. In: SPIE nano science+engineering international society for optics and photonics; 2009. 74040J–74040J-8.
[28] Smith GB. Amplified radiative cooling via optimized combinations of aperture geometry and spectral emittance profiles of surfaces and the atmosphere. Sol Energy Mat Sol Cell 2009;93(9):1696–701.
[29] Idso SB, Jackson RD. Thermal radiation from the atmosphere. J Geophys Res 1969;74:5397–403.
[30] Bliss R. Photovoltaic thermal collectors for night radiative cooling of building. Sol Energy 1961;5:103–20.
[31] Swinbank WC. Long-wave radiation from clear skies. Q J R Meteorol Soc 2007;90(89):339–48.
[32] Idso SB, Jackson RD. Thermal radiation from the atmosphere. Geophys Res 1969;74:5397–403.
[33] Brutsaert W. On a derivable formula for long-wave radiation from clear skies. Water Resour Res 1975;11:742–4.
[34] Clark G, Allen CP. The estimation of atmospheric radiation for clear and cloudy skies, in: Don Prowler, Ian Duncan (Eds.), Proceedings of Second National Passive Solar Conference 1978, Philadelphia, PA, 2:676.
[35] Idso SB. A set of equations for full spectrum and 8 to 14 mm and 10.5 to 12.5 mm thermal radiation from cloudless skies. Water Resour Res 1981;17:295–304.
[36] Berger X, Buriot D, Garnier F. About the equivalent radiative temperature for clear skies. Sol Energy 1984;32:725–33.
[37] Berdahl P, Martin M. Emissivity of clear skies. Sol Energy 1984;32:663–4.
[38] Chen H, Riffat SB, Mempouo B. Numerical study on the energy performance of a novel direct expansion PV/T heat pump. In: Proceedings of the SET2010-ninth international conference on sustainable energy technologies. Shanghai, China: s.n, 2010.
[39] Maykut GA, Church PF. Radiation climate of Barrow, Alaska, 1962–66. J Appl Meteorol 1973;12:620–8.

[40] Jacobs JD. Radiation climate of Broughton Island. In: Barry RG, Jacobs JD, editors. Energy budget studies in relation to fast-ice breakup processes in Davis Strait. Inst. of Arctic and Alp. Res. Occas. Boulder: University of Colorado; 1978.
[41] Kasten F, Czeplak G. Solar and terrestrial radiation dependent on the amount and type of cloud. Sol Energy 1980;24(2):177–89.
[42] Berdahl P, Martin M. Characteristics of infrared sky radiation in the United States. Sol Energy 1984;33(3–4):321–36.
[43] Martin M. Radiative cooling. In: Cook J, editor. Passive Cooling, s.l. Cambridge, MA: The MIT Press; 1989.
[44] Sugita M, Brutsaert W. Cloud effect in the estimation of instantaneous downward long-wave radiation. Water Resour Res 1993;29:599–605.
[45] Lhomme JP, Vacher JJ, Rocheteau A. Estimating downward long-wave radiation on the Andean Altiplano. Agric For Meteorol 2007;145:139–48.
[46] Alados-Arboledas L, Vida J, Olmo FJ. The estimation of thermal atmospheric radiation under cloudy conditions. Int J Climatol 1995;15:107–16.
[47] Niemelä S, Raisanen P, Savijarvi H. Comparison of surface radiative flux parameterizations. Part I: long-wave radiation. Atmos Res 2001;58:1–18.
[48] Crawford TM, Duchon CE. An improved parameterization for estimating effective atmospheric emissivity for use in calculating daytime downwelling long-wave radiation. Appl Meteorol 1999;38:474–80.
[49] Sugita M, Brutsaert W. Cloud effect in the estimation of instantaneous downward long-wave radiation. Water Resour Res 1993;29:599–605.
[50] Dimoudi A, Androutsopoulos A. The cooling performance of a radiator based roof component. Sol Energy 2006;80:1039–47.
[51] Erell E, Etzion Y. Radiative cooling of buildings with flat-plate solar collectors. Build Environ 2000;35(4):297–305.
[52] Meir MG, Rekstad JB, Løvvik OM. A study of a polymer-based radiative cooling system. Sol Energy 2002;73(6):403–17.
[53] Golaka A, Exell RHB. An investigation into the use of a wind shield to reduce the convective heat flux to a nocturnal radiative cooling surface. Renew Energy 2007;32(4):593–608.
[54] Raman AP, Anoma MA, Zhu L, Rephaeli E, Fan S. Passive radiative cooling below ambient air temperature under direct sunlight. Nature. 2014;515:540–4.
[55] Bathgate SN, Bosi SG. A robust convection cover material for selective radiative cooling applications. Sol Energy Mat Sol C 2011;95(10):2778–85.
[56] Bosi SG, Bathgate SN, Mills DR. At last! A durable convection cover for atmospheric window radiative cooling applications. Energy Procedia 2014;57:1997–2004.
[57] Gentle AR, Dybdal KL, Smith GB. Polymeric mesh for durable infra-red transparent convection shields: Applications in cool roofs and sky cooling. Sol Energy Mat Sol C 2013;115(10):79–85.
[58] Gentle AR, Smith GB. Optimized infra-red spectral response of surfaces for sub-ambient sky cooling as a function of humidity and operating temperature; 2010.
[59] Hay H, Yellot J. Natural cooling with roof pond and moveable insulation. ASHRAE Trans 1969;75(1):165–77.
[60] Sahar N, Kharrufa, Yahyah A. Roof pond cooling of buildings in hot arid climates. Build Environ 2008;43:82–9.
[61] Sodha MS, Singh U, Srivastava A, Tiwari GN. Experimental validation of thermal model of open roof pond. Build Environ 1981;16(2):93–8.
[62] Nahar NM, Sharma P, Purohit MM. Performance of different passive techniques for cooling of buildings in arid regions. Build Environ 2003;38:109–16.
[63] Ali AH. Passive cooling of water at night in uninsulated open tank in hot arid areas. Energy Convers Manag 2007;48:93–100.
[64] Chen B, Guenther R, Kasher J, Maloney J, Kratochvil J. Modeling of the radiative, convective and evaporative heat transfer mechanisms of the NEBRASKA modified roof pond for the determination of cooling performance curves. In: Proceedings of annual meeting of the American solar energy society. Cambridge, MA: MIT; 1988.
[65] Chen B, Guenther R, Kasher J, Maloney J, Kratochvil J, Sloup C. Cooling performance curve for the NEBRASKA modified roof pond. In: Proceedings of the combined 1987 passive solar conference and annual American solar energy society meeting. Portland, Oregon; August 1987.
[66] Roberts JD. Hybrid cooling methods—night cooldown of building mass and night-sky evaporative/radiative cooling. In: Proceedings of the second national passive solar conf. Philadelphia, vol. II; 1978. p. 657–664.
[67] Tang R, Etzion Y. Comparative studies on the water evaporation rate from a wetted surface and that from a free water surface. Build Environ 2004;3(9):77–86.
[68] Tang R, Etzion Y. On thermal performance of an improved roof pond for cooling buildings. Build Environ 2004;39:201–9.
[69] Tang R, Etzion Y, Erell E. Experimental studies on a novel roof pond configuration for the cooling of buildings. Renew Energy 2003;28:1513–22.
[70] Spanaki A, Kolokotsa D, Tsoutsos T, et al. Theoretical and experimental analysis of a novel low emissivity water pond in summer. Sol Energy 2012;86:3331–44.
[71] Spanaki A, Tsoutsos T, Kolokotsa D. On the selection and design of the proper roof pond variant for passive cooling purposes. Renew Sustain Energy Rev 2011;15:3523–33.
[72] Juchau B. Nocturnal and conventional space cooling via radiant floors. In: International Passive and Hybrid Cooling Conference. Miami Beach; 1981.
[73] Etzion Y, Erell E. Thermal storage mass in radiative cooling systems. Build Environ 1991;26(4):389–94.
[74] Saitoh TS, Fujino T. Advanced energy-efficient house (HARBEMAN house) with solar thermal, photovoltaic, and sky radiation energies (experimental results). Sol Energy 2001;70(1):63–77.
[75] Argiriou A, Santamouris M, Assimakopoulos DN. Assessment of the radiative cooling potential of a collector using hourly weather data. Energy 1994;19(8):879–88.
[76] Al-Nimr MA, Kodah Z, Nassar B. A theoretical and experimental investigation of a radiative cooling system. Sol Energy 1998;63(6):367–73.
[77] Al-Nimr MA, Tahat M, Al-Rashdan M. A night cold storage system enhanced by radiative cooling modified Australian cooling system. Appl Therm Eng 1999;19:1013–26.
[78] Erell E, Etzion Y. Analysis and experimental verification of an improved cooling radiator. Renew Energy 1999;16:700–3.
[79] Hosseinzadeh E, Taherian H. An experimental and analytical study of a radiative cooling system with unglazed flat Plate Collectors. Int J Green Energy 2012;9(8):766–79.
[80] Anderson TN, Duke M, Carson JK. Performance of an unglazed solar collector for radiant cooling. In: Proceedngs of Australian Solar Cooling 2013 Conference. Sydney.
[81] Okoronkwo CA, Nwigwe KN, Ogueke NV, Anyanwu EE. An experimental investigation of the passive cooling of a building using nighttime radiant cooling. Int J Green Energy 2014;11(10):1072–83.
[82] Tevar JAF, Castaño S, Marijuán AG, Heras MR, Pistono J. Modeling and experimental analysis of three radioconvective panels for night cooling. Energy Build 2015;107(15):37–48.
[83] Givoni B. Solar heating and night radiation cooling by a roof radiation trap. Energy Build 1977;1(2):141–5.
[84] Mihalakakou G, Ferrante A, Lewis JO. The cooling potential of a metallic nocturnal radiator. Energy Build 1998;28:251–6.
[85] Bagiorgas HS, Mihalakakou G. Experimental and theoretical investigation of a nocturnal radiator for space cooling. Renew Energy 2008;33(6):122–7.
[86] Khedari J, Waewsak J, Thepa S, Hirunlabh J. Field investigation of night radiation cooling under tropical climate. Renew Energy 2000;20(2):183–93.
[87] Parker DS. Theoretical evaluation of the NightCool nocturnal radiation cooling concept. Submitted to Us Department of Energy Fsec; 2005.
[88] Parker DS, Sherwin JR. Evaluation of the NightCool nocturnal radiation cooling concept: annual performance assessment in scale test buildings. Submitted to Us Department of Energy Fsec; 2008.
[89] Hollick J. Nocturnal radiation cooling tests. Energy Procedia 2012;30(1):930–6.
[90] Conserval Engineering Inc. NightSolar solar cooling system. ⟨http://solarwall.com/en/ products/ nightsolar-air-cooling.php⟩.
[91] Falt M, Zevenhoven M. Radiative cooling in Northern Europe using a skylight. J Energy Power Eng 2011:692–702.
[92] Eicker U, Dalibard A. Photovoltaic–thermal collectors for night radiative cooling of buildings. Sol Energy 2011;85(7):1322–35.
[93] Sohel MI, Ma Z, Cooper P, Adams J, Niccol L. A feasibility study of night radiative cooling of BIPVT in climatic conditions of major Australian cities. In: Proceedings of Asia-Pacific solar research conference; 2014.
[94] Fiorentini M, Cooper P, Ma Z. Development and optimization of an innovative HVAC system with integrated PVT and PCM thermal storage for a net-zero energy retrofitted house. Energy Build 2015;94:21–32.
[95] Lin W, Ma Z, Sohel MI, Cooper P. Development and evaluation of a ceiling ventilation system enhanced by solar photovoltaic thermal collectors and phase change materials. Energy Convers Manag 2014;88:218–30.
[96] Zhang S, Niu J. Cooling performance of nocturnal radiative cooling combined with microencapsulated phase change material (MPCM) slurry storage. Energy Build 2012;54(8):122–30.
[97] Heidarinejad G, Farahani MF, Delfani S. Investigation of a hybrid system of nocturnal radiative cooling and direct evaporative cooling. Build Environ 2010;45(45):1521–8.
[98] Farahani MF, Heidarinejad G, Delfani S. A two-stage system of nocturnal radiative and indirect evaporative cooling for conditions in Tehran. Energy Build 2010;42(11):2131–8.
[99] Ezekwe CI. Performance of a heat pipe assisted night sky radiative cooler. Energy Convers Manag 1990;30(4):403–8.
[100] Chotivisarut N, Kiatsiriroat T. Cooling load reduction of building by seasonal nocturnal cooling water from thermosyphon heat pipe radiator. Int J Energy Res 2009;33(12):1089–98.
[101] Chotivisarut N, Nuntaphan A, Kiatsiriroat T. Seasonal cooling load reduction of building by thermosyphon heat pipe radiator in different climate areas. Renew Energy 2012;38(1):188–94.
[102] Lu SM, Yan WJ. Development and experimental validation of a full-scale solar desiccant enhanced radiative cooling system. Renew Energy 1995;6(7):821–7.
[103] Ali AHH. Desiccant enhanced nocturnal radiative cooling-solar collector system for air comfort application in hot arid areas. Sustain Energy Technol Asses 2013;1:54–62.
[104] Cui Y, Wang Y, Zhu L. Performance analysis on a building-integrated solar heating and cooling panel. Renew Energy 2015;74:627–32.
[105] Man Y, Yang H, Spitler JD, Fang Z. Feasibility study on novel hybrid ground coupled heat pump system with nocturnal cooling radiator for cooling load dominated buildings. Appl Energy 2011;88(11):4160–71.
[106] Zingre KT, Wan MP, Tong S, et al. Modeling of cool roof heat transfer in tropical climate. Renew Energy 2015;75(75):210–23.
[107] Hodo-Abalo S, Banna M, Zeghmati B. Performance analysis of a planted roof as a passive cooling technique in hot-humid tropics. Renew Energy 2012;39(1):140–8.
[108] Santamouris M, Synnefa A, Karlessi T. Using advanced cool materials in the urban built environment to mitigate heat islands and improve thermal comfort conditions. Sol Energy 2011;85:3085–102.

[109] Kolokotsa D, Santamouris M, Zerefos SC. Green and cool roofs' urban heat island mitigation potential in European climates for office buildings under free floating conditions. Sol Energy 2013;74:118–30.
[110] Gentle AR, Aguilar LC, Smith GB. Optimized cool roofs: Integrating albedo and thermal emittance with R-value. Sol Energy Mat Sol C 2011;95(12):3207–15.
[111] Aubrey J. Cool Roof [Online]; 2010. Available from: ⟨http://people.csail.mit.edu/ jaffer/cool/CoolRoof⟩.
[112] Miller W, Crompton G, Bell J. Analysis of cool roof coatings for residential demand side management in tropical Australia. Energies 2015;8:5303–18.
[113] Gentle AR, Smith GB. A subambient open roof surface under the mid-summer sun. Adv Sci 2015;2:9.
[114] Muselli M. Passive cooling for air-conditioning energy savings with new radiative low-cost coatings. Energy Build 2010;42(6):945–54.
[115] Taleghani M, Tenpierik M, Dobbelsteen AVD, et al. Heat mitigation strategies in winter and summer: field measurements in temperate climates. Build Environ 2014;81(11):309–19.
[116] Min HC, Jin CP, Ko MJ. Effect of the solar radiative properties of existing building roof materials on the energy use in humid continental climates. Energy Build 2015;102:172–80.
[117] Berdahl P. Selective radiative cooling with MgO and LiF layers. Appl Opt 1984;23(3):370–2.
[118] Catalanotti S, Cuomo V, Piro G, Ruggi D, Silvestrini V, Troise G. The radiative cooling of selective surfaces. Sol Energy 1975;17:83–9.
[119] Nilsson TMJ, Niklasson GA, Granqvist CG. A solar reflecting material for radiative cooling applications: ZnS pigmented polyethylene. In: Proceedings of SPIE - the international society for optical engineering. vol. 28, 92; 1992: p. 175–193.
[120] Nilsson TMJ, Niklasson GA. Radiative cooling during the day: simulations and experiments on pigmented polyethylene cover foils. Sol Energy Mater Sol C 1995;37(1):93–118.
[121] Dobson KD, Hodes G, Mastai Y. Thin semiconductor films for radiative cooling applications. Sol Energy Mat Sol C 2003;80(3):283–96.
[122] Michell D, Biggs KL. Radiation cooling of buildings at night. Appl Energy 1979;5(79):263–75.
[123] Bartoli B, Catalanotti S, Coluzzi B, et al. Nocturnal and diurnal performances of selective radiators. Appl Energy 1977;3(4):267–86.
[124] Harrison AW, Walton MR. Radiative cooling of TiO_2 white paint. Sol Energy 1978;20(2):185–8.
[125] Eriksson TS, Jiang SJ, Granqvist CG. Surface coatings for radiative cooling applications - silicon dioxide and silicon nitride made by reactive RF-sputtering. Sol Energy Mater 1985;12(85):319–25.
[126] Diatezua MD, Thiry PA, Caudano R. Characterization of silicon oxynitride multilayered systems for passive radiative cooling application. Vacuum 1995;46(8):1121–4.
[127] Martin M, Berdahl P. Summary of results from the spectral and angular sky radiation measurement program. Sol Energy 1984;33(84):241–52.
[128] Ezekwe CI. Nocturnal radiation measurements in Nigeria. Sol Energy 1986;37(1):1–6.
[129] Ito S, Miura N. Studies of radiative cooling systems for storing thermal energy. J Sol Energy Eng 1989;3(3):251–6.
[130] Dobson RT. Thermal modelling of a night sky radiation cooling system. J Energy S Afr 2005;16(2):20–31.
[131] Erell E, Etzion Y. A radiative cooling system using water as a heat exchange medium. Archit Sci Rev 1992;35(2):39–49.
[132] Rincón J, Almao N, González E. Experimental and numerical evaluation of a solar passive cooling system under hot and humid climatic conditions. Sol Energy 2001;71(1):71–80.
[133] Al-Zubaydi AYT, Dartnall WJ. Design and modelling of water chilling production system by the combined effects of evaporation and night sky radiation. J Renew Energy 2014.
[134] Effects of the passive use of nocturnal radiative cooling in fresh vegetable cooling. Japan: NIRE, National Institute for Rural Engineering; 2000.
[135] Zhu L, Fan S. Near-complete violation of detailed balance in thermal radiation. Phys Rev B 2014;90(22).
[136] N. Fernandez, W. Wang, K. Alvine and S. Katipamula, Energy savings potential of radiative cooling technologies, 2015, Pacific Northwest National Laboratory; Richland, WA 10.2172/1234791.
[137] Hossain MM, Gu M. Radiative cooling: principles, progress, and potentials. Adv Sci 2016.
[138] Levinson R, Akbari H. Potential benefits of cool roofs on commercial buildings: conserving energy, saving money, and reducing emission of greenhouse gases and air pollutants. Energy Effic 2010;3(1):53–109.
[139] Hosseini M, Akbari H. Effect of cool roofs on commercial buildings energy use in cold climates. Energ Build 2015;114:143–55.
[140] Yannas S, Erell E, Molina JL. Roof cooling techniques: a design handbook. London: Earthscan; 2006.
[141] Enderlin AR. Radiative cooling to the night sky.Fayetteville, AR: University Of Arkansas; 2015.
[142] Collins T, Parker S. Technology installation review: whitecap roof spray cooling system.Richland, WA: Pacific Northwest National Laboratory; 1998. ⟨http://www.builditsolar.com/Projects/Cooling/WhitecapRoofCoolingReport.pdf⟩.
[143] Oak Ridge National Laboratory. "Night Sky" system cools roof tops, saves energy 2014. ⟨http://web.ornl.gov/sci/eere/international/Website/Nightsky%20Cools%20RoofTops.htm⟩.